# NASA CONTRACTOR REPORT

NASA CR-2033

NASA CR-2

c. 1

# MODELS OF GRAVITY WAVE PERTURBATIONS OF THE NEUTRAL UPPER ATMOSPHERE OF THE EARTH

*by* Ganti L. Rao

TECH LIBRARY KAFB, NM

0061327

| 1. REPORT NO.<br>CR-2033 | 2. GOVERNMENT ACCESSION NO. | 3. RECIPIENT'S CATALOG NO. |
|---|---|---|
| 4. TITLE AND SUBTITLE<br><br>MODELS OF GRAVITY WAVE PERTURBATIONS OF THE NEUTRAL UPPER ATMOSPHERE OF THE EARTH | | 5. REPORT DATE<br>April 1972 |
| | | 6. PERFORMING ORGANIZATION CODE |
| 7. AUTHOR(S)<br>Ganti L. Rao | | 8. PERFORMING ORGANIZATION REPORT # |
| 9. PERFORMING ORGANIZATION NAME AND ADDRESS<br>Columbia University<br>Lamont-Doherty Geological Observatory<br>Palisades, New York 10964 | | 10. WORK UNIT NO. |
| | | 11. CONTRACT OR GRANT NO.<br>NAS8-27088 |
| | | 13. TYPE OF REPORT & PERIOD COVERED |
| 12. SPONSORING AGENCY NAME AND ADDRESS<br><br>NASA<br>Washington, D. C. 20546 | | CONTRACTOR REPORT |
| | | 14. SPONSORING AGENCY CODE |

15. SUPPLEMENTARY NOTES

Project Managers: Harold C. Euler and Robert E. Smith, Aerospace Environment Division, Aero-Astrodynamics Laboratory, Marshall Space Flight Center, Alabam 35812

16. ABSTRACT

Observational data from an array of CW Doppler sounding stations were analyzed and traveling ionospheric disturbances (TID's) were identified and analyzed using spectral analysis techniques. Seasonal variations in frequency, direction and speed of propagation of TID's were found which could be explained as manifestations of internal acoustic gravity waves where propagation was influenced by the thermodynamic structure of the mesosphere and lower thermosphere.

| 17. KEY WORDS<br><br>1. Gravity Waves<br>2. Doppler effect<br>3. Upper Atmosphere<br>4. Ionospheric disturbances | | 18. DISTRIBUTION STATEMENT | | |
|---|---|---|---|---|
| 19. SECURITY CLASSIF. (of this report)<br>Unclassified | 20. SECURITY CLASSIF. (of this page)<br>Unclassified | | 21. NO. OF PAGES<br>65 | 22. PRICE<br>$3.00 |

# Table of Contents

FOREWORD

This report was prepared by Lamont-Doherty Geological
Observatory of Columbia University under contract number
NAS8-27088, "Models of Gravity Wave Perturbations of the
Neutral Upper atmosphere of the Earth" for the George C.
Marshall Space Flight Center of the National Aeronautics and
Space Administration.  The work was administered under the
technical direction of the Aero-Astrodynamics Laboratory of
the George C. Marshall Space Flight Center with Harold C.
Euler and Robert E. Smith acting as project managers.

## Introduction:

The dynamical behavior of the upper atmosphere produces several phenomena, such as wave forms in noctilucent clouds, irregular structure in wind systems near the base of the thermosphere, and variations in the vertical temperature structure profiles. These phenomena are partly accounted as manifestations of internal atmospheric gravity waves (Hines 1960).

The electron density distribution in the ionosphere exhibits perturbations of varying intensities and spatial dimensions. If one considers the medium as a series of isoionic contours of constant ion density, then the presence of such perturbations produces curvatures and tilts of these surfaces, resulting in diffraction, refraction and reflection processes of radio waves traversing in the medium. When these disturbances travel horizontally in the ionosphere their radiowave pattern on the ground moves correspondingly. These disturbances are broadly classified as travelling ionospheric disturbances or TIDs and they frequently appear in the form of propagating wave-like motions ranging in magnitude from very large scale disturbances with periods of the order of an hour that travel thousands of kilometers (Chan and Villard, 1962) to wave effects with periods near one minute probably locally generated (Davies and Baker, 1969).

Between these extremes are types of wavelike motions with periods in the range of 8 minutes to 1 hour and phase velocities 50-200 m.sec$^{-1}$ called "medium scale" disturbances which occur frequently and have been widely observed.

Travelling ionospheric disturbances have been studied for many years by a variety of techniques but it is only recently that a theory has been advanced which appears to fit the available experimental data. This is the acoustic-gravity wave theory in which the observed electron density perturbations are attributed due to acoustic gravity waves.

Earlier work on TIDs provided information on speeds and directions. A clear description of wave characteristics such as periods and wavelengths is not available and it is this problem which is investigated here. CW doppler data is analyzed to provide a statistical description of the wave characteristics of medium scale TIDs. For some TID events both horizontal and vertical velocities are computed to investigate wavefront tilts. Long period sound waves generated by Saturn-Apollo launches recorded on doppler sounders and ionograms are analyzed and inter-preted. TID characteristics are investigated and an apparent correlation between TIDs and occurrence of sporadic E has been examined in the light of internal

atmospheric gravity theory concepts. The results of this work were compared with those of earlier investigations. A summary of the results and suggestions for future work were presented at the end of the report.

2. Earlier Work on TID's

Pierce and Mimno (1940) were the first investigators to notice the presence of TIDs in the F2 region of the ionosphere. From comparatively little evidence they built up a description of the disturbance as observed at one receiving site. Later, Wells et al (1946) found evidence which led them to believe that a vertical transport of ionization clouds exists in the F2 region. TIDs were also studied by Beynon (1948) during sunrise and between 1900-0500 LMT in the winter of 1942-43. The average speed reported by him was 120 m sec$^{-1}$ and the direction of travel was westward during sunrise hours. Munro (1950, 1953a,b, 1958) suggested that these wave-like disturbances seen on ionograms may be due to the disturbances in the neutral atmosphere itself, taking the form of travelling pressure waves which cause a redistribution of ionization. These quasi-periodic changes of the electron density, especially in the F2 region, were explained by Martyn (1950) as being due to horizontally travelling atmospheric cellular waves of the type investigated by Lamb (1909). Beynon and Thomas

(1954) found that an increase in TID phase velocity was
followed by an increase in geomagnetic K index. Munro's
experiments were repeated at Perth, West Australia by
Price during the daytime in winter and summer of 1950-1952.
The results of this experiment (Price, 1953, 1955) indicated
that the phase velocities ranged from 90-330 m sec$^{-1}$ and
that the direction of travel varied from $0^{\circ}$ to $60^{\circ}$E of N
during winter and in the range $90^{\circ}$ to $180^{\circ}$E of N during
summer. Bramley and Ross (1951) and Bramley (1953) used
the same technique, and obtained velocities in the range
35-330 m sec$^{-1}$. Sen (1949) and Osborne (1955) in Singapore,
and Skinner et al (1954) in Ibadan also observed perturbations
in H. F. records at low latitudes which they attributed to
TIDs.

Using vertical incidence soundings of the ionospheric
F2 regions from an array of three stations separated 200 km
apart, Thomas (1959) obtained velocities of propagation by
studying corresponding fluctuations in the critical frequency
and the equivalent height of reflection, at a particular
height, on all three stations. The measured velocities
ranged from 40-280 m sec$^{-1}$ and the direction of travel was
mainly SE. Using another station at 650km from the main array,
he showed that TIDs travelled with little change in direction

and speed.  He obtained a positive vertical gradient of
1 m sec$^{-1}$/km of velocity within the F2 region.  The vertical
gradient was larger in winter than in summer.

Many investigators have reported the existence of
large travelling disturbances (TIDs) detected by such
methods as vertical soundings, doppler phase-path soundings
and H.F. backscatter techniques.  Castel and Faynot (1964),
utilizing simultaneous observations from ground network
of rapid sequence ionosondes and topside soundings from the
Alouette Satellite, detected large disturbances usually
moving southward with an apparent speed of 180 m sec$^{-1}$.
They further postulated that these irregularities originate
at high latitudes and move toward equatorial regions.  From
the occurrence of irregularities in the Faraday rotation
period of satellite signals, Liszka and Taylor (1965)
presented some tentative evidence that large irregularities
in total electron content, which occur in patches with
horizontal scales of 1000 km, may be generated in the auroral
zone and then propagate southward with velocities of a few
hundred meters per second.  Recently, Thome (1964) and Thome
and Rao (1968) have reported the results of a study of large
scale travelling disturbances in the ionosphere using a
combination of incoherent back-scatter sounding technique

and phase-path doppler technique. They concluded that the large TIDs were propagated by atmospheric gravity waves and that the auroral electrojet was the most probable energy source. Hunsucker and Tveten (1967) reported large TIDs using high-resolution H.F. backscatter sounder. The direction of motion was predominantly toward the southeast and the horizontal speeds were in the range 100-170 m sec$^{-1}$. A summary of TID investigations is presented in Table 1.

Table 1

TID Observations

| Investigator | Technique | Speed | Comments |
|---|---|---|---|
| 1. Bowman (1965) | Ionosonde | 361m/sec 722m/sec (assumed) | Reports sources as conjugate high-latitude locations. TIDs occurred following SCs. |
| 2. Chan & Villard (1964) | Cw Doppler | 400-765m/sec | TIDs occurred following SCs. |
| 3. Castel & Faynot (1964 | Satellite signals | 180m/sec | Simultaneous upper and lower ionospheric data. Suggest high-latitude origin |
| 4. Georges (1968) | Cw Doppler | Two groups: <300m/sec, >300m/sec | Medium scale and very large TIDs. From north. |
| 5. Goodwin (1968) | Ionosonde | 30m/sec | Large-scale irregularities in F region. Suggests origin near geomagnetic pole |
| 6. Heisler (1958) | Ionosonde | 97-207m/sec | Followed TIDs 3000km from Hobart to Townsville |
| 7. Hunsucker & Tveten (1967) | High-resolution HF backscatter | 82-325m/sec | 52% preceded by auroral activity at suitable time for auroral origin. |

7

| Investigator | Technique | Speed | Comments |
|---|---|---|---|
| 8. King (1966) | Ionosonde | 200m/sec | Accepts infrasonic evidence as to auroral source. |
| 9. Liszka & Taylor (1965) | Faraday rotation of satellite signals | 200-300m/sec | Suggest auroral zone source |
| 10. Munro (1958) | Three 5.8 MHz pulsed transmitters | 120-150m/sec | Waves come from winter polar region. Nine years of data. |
| 11. Thome (1966) | Thomson backscatter sounder at Arecibo, f-430MHz | 50-100m/sec | Suggests auroral electrojet as source. |
| 12. Titheridge (1968) | Faraday rotation or polarization of satellite signals | 50m/sec | Waves in New Zealand travelled towards the north. |
| 13. Wright (1961) | Ionosonde | 406-691m/sec | Followed TIDs 1100 km from Campbell Island to Christchurch. |
| 14. Davies & Jones (1971) | Cw Doppler Sounder | 120-170m/sec | Waves from winter polar region. |

## 3. TID observations and CW doppler array

TIDs in the ionized regions of the earth's atmosphere have been observed by various methods. Among the frequently employed methods are conventional ionosondes, incoherent backscatter, high frequency ground backscatter radar and phase sounders. There are two kinds of phase sounders. One uses pulse sounding and the other uses Cw sounding. In the present investigation of TIDs an array of Cw doppler sounders were used to monitor and record several TIDs of various characteristics.

The doppler system was built similar to Davies' system (Davies 1962, Davies and Baker 1965). A significant difference between Davies system and the present system is in the presentation of data. In our system the doppler signal is digitized and stored in digital magnetic tape whereas in the Davies system the signal is recorded in analog form. The digital form of recording of data allows the use of modern digital processing techniques such as cross correlation, power and cross spectral analyses, digital filtering and contour plotting. The sensitivity of the doppler technique in its present state of development is about 0.1 Hz, that is phase-path changes as small as 1/10 of a radiowave length per second can be measured. At 4 MHz this corresponds to $dp/dt \simeq 7.5$ m.sec$^{-1}$.

9

## 4. Data and Method of Analyses

CW doppler data taken from October 1969 - February 1970 were characterized by certain events which represent a distinct class of travelling ionospheric disturbance. These events have a quasi-period range from 8 min to 24 min, the doppler frequency shifts are 1 to 4 Hz peak to peak, and the disturbances usually exhibit two and three sinusoidal cycles that are shifted in time on the traces corresponding to the various radio paths. For detection and further detailed analysis of TID signatures over a background doppler variation the following criteria was adopted.

(1) All radio transmission signals should be reflected from the same reflecting height. In this case the reflections are from F region of the ionosphere.

(2) Similar characteristics and periods should be seen on all the channels.

(3) Signal to noise ratio should be good in all the channels.

When computing the propagation characteristics of TID care should be exercised in selecting the time window for computing cross correlation coefficients. A good statistical estimate of the parameters can be obtained by taking large time windows. On the other hand, the ionosphere is dynamic in nature and large diurnal variations are often

noticed on electron density perturbations, and as such the
time windows should not be too large to include the diurnal
changes.  In the case of medium scale TIDs the signature
(or signal) lasted between 2 to 5 hours.  For periods between
10-20 minutes, about a 2-hour window seems to give a good
estimate of cross correlation coefficients for each two-hour
window.  If the phase velocities for all the windows for
an event were within reasonable agreement ($\pm$ 15 m sec$^{-1}$),
then an average phase velocity for the event was computed,
otherwise it was rejected.

The cross correlation functions $\rho_{34}$, $\rho_{35}$ and $\rho_{45}$
between the station pairs Catskill-Thornhurst, Catskill-
Westwood and Thornhurst-Westwood respectively, were computed.
The phase velocity was calculated from the following
equations using the station geometry as shown in Figure 1,
and the time delays derived from the cross correlation
analysis

$$\tan \Theta = \left(\frac{\chi_{34}}{\chi_{35}}\right)\left(\frac{\tau_{35}}{\tau_{34}}\right) \frac{1}{\sin \alpha} =\ \psi \circ \tau \ a$$

$$V = \left(\frac{\chi_{34}}{\tau_{34}}\right) \cos \Theta = \left(\frac{\chi_{35}}{\tau_{35}}\right) \cos (\alpha - \Theta)$$

where

$\chi_{34}$ and $\chi_{35}$ are the ionospheric reflection point distances
between stations Catskill-Thornhurst and Catskill-Westwood
respectively, $\tau_{34}$ and $\tau_{35}$ are the corresponding time delays,

11

α is the angle between the paths joining Catskill-Thornhurst and Catskill-Westwood,

Θ is the direction of propagation of the disturbance measured anti-clockwise from the line joining the stations Catskill-Thornhurst, and V is the estimate of the horizontal phase velocity.

Some of the TID events were subjected to power and cross spectral analyses. The general problem of spectrum analyses of digital samples was formulated by Blackman and Tukey (1959). Their method of obtaining the estimates of the power and cross power spectral densities has been followed.

Consider the cross correlation function of two time series (Lee. 1960).

$$\rho_{12}(\tau) = \lim_{T \to \infty} \frac{1}{T} \int_{-T/2}^{T/2} f_1(t) f_2(t+\tau) dt \qquad (1)$$

where $f_1(t)$ and $f_2(t)$ are the two time series, T is the record length and $\tau$ is the time lag of $f_1$ relative to $f_2$. In the special case when $f_1 = f_2$ equation (1) becomes the correlation function

$$\rho_{11}(\tau) = \lim_{T \to \infty} \frac{1}{T} \int_{-T/2}^{T/2} f_1(t) f_2(t+\tau) dt \qquad (2)$$

The power density spectrum and the cross density spectrum are given by Fourier – transforming the auto and cross correlation functions respectively.

12

$$P_{11}(\omega) = \frac{1}{2\pi} \int\limits_{-\infty}^{+\infty} \rho_{11}(\tau)\bar{e}^{i\omega\tau}dt \tag{3}$$

$$P_{12}(\omega) = \frac{1}{2\pi} \int\limits_{-\infty}^{+\infty} \rho_{12}(\tau)\bar{e}^{i\omega\tau}dt \tag{4}$$

where $\omega$ is the angular frequency in radians per unit time.
In general the cross-correlation function is assymmetrical
and the cross spectrum therefore is complex.

$$P_{12}(\omega) = C_o(\omega)+iQuad(\omega), \tag{5}$$

where $C_o(\omega)$ is the real part and $Quad(\omega)$ the imaginary part.

The phase relationship between frequencies, in records
being cross-spectrum analysed is given by

$$\Delta\Theta(\omega) = \Theta_2(\omega)-\Theta_1(\omega) = \tan^{-1}\left[\frac{Quad(\omega)}{C_o(\omega)}\right] \tag{6}$$

$\Theta_1(\omega)$ = phase of time series $f_1(t)$

$\Theta_2(\omega)$ = phase of time series $f_2(t)$

The coherence estimates were obtained from the definition

$$\left|\gamma(i\omega)\right|^2 = \frac{\left|P_{12}(\omega)\right|^2}{P_{11}(\omega).P_{22}(\omega)} \tag{7}$$

where
$\gamma(i\omega)$ = magnitude of the complex coherence.
The amplitude of the cross spectrum at each frequency is
the product of the corresponding amplitudes in the two tome
series. If a particular spectral component is absent from
either series, it will be absent from the cross-spectrum,

and the coherence will be a minimum at that frequency.

Blackman and Tukey (1959) have recommended that in order to minimize leakage from the low frequencies into the high frequencies, the data should be pre-whitened prior to the power spectrum analysis. This has been accomplished in this work by applying to the data a simple derivative filter.

The smoothed spectral estimates were obtained using a "hanning window" which has side lobes of the order of 1% of the main lobe. The number of lags was equal to 10% of the data sample giving 20 degrees of freedom.

The lowest frequency that can be analyzed in the data sample is determined by the maximum lag, Tm, since $fmin = (2Tm)^{-1}$. The digitizing interval, $\Delta t$, determines the highest frequency, $fmax = (2\Delta t)^{-1}$.

The pre-whitening filter and the electric filter of the data acquisition system, were restored by multiplying each spectral estimate by the inverse of the square of the amplitude response at that frequency.

## 5. Results of the present Investigation:

For all the TID events taken during the period September 1969 through April 1970, the horizontal phase velocity and direction have been computed. Typical TIDs are shown in figures 2 through 6. The velocities of all TID events were plotted against local time (Eastern Standard time) as shown in the figure 7. It can be seen that most of the TID events occurred between 0600-1000 and 1400-2000 hours local time. These times correspond to post sunrise, sunset and post sunset conditions. It can also be noticed from the figure that the horizontal phase speeds of TIDs during midnight conditions are high compared to daytime and sunset time TID events. The directions of all TIDs have also been plotted against local time, as shown in figure 8, to study the diurnal variation of the direction heading of TIDs. During the local times 1500-2000 where TID activity seems to be predominant, the TID directions also appear to be consistent. The direction in which TIDs were heading during this interval of time was southwest to west. During the morning hours the predominant direction seems to be southeast and toward north during night time conditions.

Histograms for TID velocities for 20 m.sec$^{-1}$ intervals were drawn as shown in figure 9. It can be seen from the figure that the histograms peaks for intervals between

100-180 m.sec$^{-1}$. Histograms for TID directions for 20$^{\circ}$ intervals were also drawn as shown in figure 10. From the histogram it can be seen that the direction of heading of TIDs was in the intervals 120$^{\circ}$-140$^{\circ}$ (measured east of north) and 200$^{\circ}$-240$^{\circ}$. This investigation shows that the medium scale TIDs have phase velocities in the range 60-200m.sec$^{-1}$ and the predominant direction of travel is between SE to SW. Higher magnitudes of velocities of the order of 400$\sim$500 m.sec$^{-1}$ are noticed during night time travelling toward north.

Munro (1950) from an extensive study on daytime medium scale TIDs from southern hemisphere station reported that the mean direction of travel was approximately 20$^{\circ}$(E of N) for winter conditions and approximately 11$^{\circ}$(E of N) for summer conditions. The horizontal speeds varied from 85-170m.sec$^{-1}$. The following conclusions regarding the directions of medium scale TIDs may be drawn from the results of the present investigation and those of the earlier results (Munro, 1950, Chan and Villard, 1962; Georges 1968; Davies and Jones, 1971)

1. During summer and winter seasons, TIDs in northern and southern hemispheres travel away from the winter pole

2. During spring and fall seasons, TIDs in northern hemisphere have predominant westward direction while those in southern hemisphere have predominant eastward direction.

# 6. Three Dimensional Observations of TIDs:

The results reported in the earlier section were mainly derived from an array of CW doppler sounders operating at 48 MHz. During winter of 1969-70 another doppler sounder was operated at 6 MHz from Westwood to study both the horizontal and vertical components of the TIDs.

The horizontal and vertical components of the velocities were determined for 18 samples by the methods outlined in previous section. The vertical spacing between 4.8 MHz and 6.0 MHz reflected signals were obtained using Wallops Islands ionograms. For the winter ionospheric conditions for Wallops Islands the vertical spacing for 4.8 MHz and 6.0 MHz signals varied between 12 to 15 km depending upon the local ionospheric conditions during the passage of a TID.

The number of TID events suitable for analysis was limited to 18 for the following reasons. Most of the observations were limited to daytime and sunset conditions because only then the 4.8 and 6.0 MHz signals reflected from the F2 region. Analysis of the night time signals were not possible as most of the time 6.0 MHz signal either went into saturation or lost into space. Only events which are visually similar were selected for analysis to increase the probability that the disturbance was produced by a single dominant atmospheric wave.

The three dimensional TID velocity vector is expressed in spherical co-ordinates, where V represents velocity in m.sec$^{-1}$. $\Phi$ the azimuth in degrees measured east of north and $\psi$ the inclination in degrees above the horizontal. The results of the analysis of the three dimensional TIDs are presented in Table 2. The TID periods were obtained from spectral analysis as outlined in earlier section.

It can be seen from the table 2 that in all cases the disturbances have a downward direction. Histograms for $\psi$ for $10^{\circ}$ intervals were drawn as shown in figure 11 and the histograms peaks in the intervals $40^{\circ}-70^{\circ}$ with a mean value of $57^{\circ}$. The velocity varied from 27m.sec$^{-1}$ to 112 m.sec$^{-1}$ with a mean value of 65 m.sec$^{-1}$. As can be seen from figure 12 the azimuth in winter is towards south.

The three dimensional TID results using CW doppler technique are available from Boulder $(40^{\circ})$. The true velocities reported by Davies and Jones (1971) from Boulder varied from 83 to 224 m.sec$^{-1}$ with a mean value of 143 m.sec$^{-1}$. This value is higher than the value reported in the present investigation. The reason for this is that the results of the present study are mostly daytime values whereas Davies and Jones (1971) observations are for sunset and night time conditions. The night time values are usually higher than the daytime values.

The azimuth and the inclination of the velocity vector are
in general agreement with Davies and Jones (1971) findings.

The significance of the results presented in this section
are examined in the light of atmospheric gravity wave concepts
in the next section.

# TABLE 2

## Three Dimensional TID Observations for the Winter 1969

| Date | Time(EST) | $V(m.sec^{-1})$ | $\Phi^\circ$ | $\psi^\circ$ | Tmin | $\lambda km$ | Theoretical Values $\psi$ $t_B=10.5$ | $\psi$ $t_B=14$ |
|------|-----------|------|------|------|------|------|------|------|
| 11-15-69 | 0700 | 71 | 135 | $-54^\circ$ | 20 | 85 | -58 | -45 |
| 11-28-69 | 1400 | 29 | 122 | $-76^\circ$ | 16 | 28 | -49 | -29 |
| 11-29-69 | 1400 | 29 | 254 | $-73^\circ$ | 20 | 35 | -58 | -45 |
| 11-29-69 | 1800 | 95 | 164 | $-43^\circ$ | 18 | 104 | -54 | -39 |
| 11-30-69 | 1600 | 65 | 205 | $-70^\circ$ | 21 | 82 | -60 | -48 |
| 11-30-69 | 2000 | 64 | 228 | $-66^\circ$ | 21 | 81 | -60 | -48 |
| 12-1-69 | 1630 | 112 | 213 | -43 | 36 | 245 | -73 | -67 |
| 12-2-69 | 1630 | 86 | 210 | -43 | 36 | 186 | -73 | -67 |
| 12-3-69 | 0700 | 61 | 337 | -46 | 24 | 88 | -64 | -54 |
| 12-3-69 | 1700 | 96 | 201 | -49 | 36 | 207 | -73 | -67 |
| 12-5-69 | 0900 | 58 | 240 | -42 | 12 | 42 | -29 | |
| 12-5-69 | 1800 | 52 | 213 | -69 | 19 | 59 | -56 | -47 |
| 12-6-69 | 0800 | 77 | 209 | -67 | 24 | 111 | -64 | -54 |
| 12-17-69 | 1430 | 67 | 129 | -53 | 10 | 40 | | |
| 12-18-69 | 0100 | 225 | 192 | -67 | 17 | 229 | -52 | -34 |
| 12-18-69 | 1100 | 61 | 117 | -30 | 24 | 46 | -64 | -54 |
| 12-20-69 | 1100 | 72 | 331 | -56 | 15 | 65 | -46 | -7 |

## 7 TIDs and Internal Atmospheric Gravity Waves:

TIDs have been observed by several techniques by various investigators. However, it is still not clear what is the general nature of the travelling disturbance mechanism. It may be argued that winds in F-region levels may act as transport mechanism. Winds at F region heights are not capable of moving ionization across geomagnetic field lines with any appreciable efficiency but they do impart to the ionization their component of velocity in the direction of the geomagnetic field. Horizontal winds moving with the speeds observed would thereby tend to raise or lower the whole F layer but no such unidirectional motion is observed. The vertical motion could be diminished by the effects of vertical polarization fields generated by the motion itself, but the degree of diminuation is not appreciable at most latitudes. This shows that it is justified to argue against atmospheric winds as the transport mechanism.

Hydromagnetic waves of pertinent periods are likely to be strongly absorbed in the F region but these waves can probably be discounted on the basis of speed as they travel much faster than the observed disturbances. The Alfrén speed at 250 km is about 3300 m.sec$^{-1}$ (Hines 1960, Ovezgel'dyyer and Lezhneva, 1965). The chief attraction

of the hydromagnetic hypothesis was its ability to explain
the apparent downward progression of the disturbances as
a direct consequence of generation at great height.  This
conflicts with experimental observation which indicated
that disturbances in the F1 region are often not to be
found in F2 region above (Heisler 1958).

Internal atmospheric gravity waves do appear to have
the necessary characteristics to account for the behavior
of travelling ionospheric disturbances (Hines 1960).  For
an isothermal atmosphere at a height of 225 km the shortest
period of these oscillations would be around 10-15 min.
If the energy of the wave were propagating upwards into F
region then it will ultimately be dissipated when viscous
effects become large.

The basic equations that govern the propagation of the
acoustic gravity waves in an isothermal tamosphere with
viscous forces taken into account are given by Pitteway
and Hines (1963) as:

$$\rho_0\frac{\partial \vec{u}}{\partial t} = \rho\vec{g}-\nabla p+(\nabla \cdot \mu\nabla)\vec{u}+\nabla(\mu\nabla \cdot \vec{u})/3+(\nabla\mu x\vec{v})x\vec{u} \qquad (1)$$

$$\frac{\partial p}{\mu t}+\vec{u}\cdot\nabla p_0 = C^2(\frac{\partial \rho}{\partial t}+\vec{u}\cdot\nabla \rho_0) \qquad (2)$$

$$\frac{\partial \rho}{\partial t}+\nabla\cdot(\rho_0\vec{u}) = 0 \qquad (3)$$

Various symbols in these and the following equations are the same as defined by Hines (1960) and Hines and Pitteway (1963). Assuming that the deviations in pressure, density and the velocity from the ambient are of perturbation magnitude, we seek the wave solutions for the above equations in complex Fourier form such that

$$\frac{p'}{p_o p} = \frac{\rho'}{\rho' R} = \frac{U_x}{X} = \frac{U_z}{Z} = A \exp i(\omega t - K_x x - K_z z)L \qquad (4)$$

where $p' = p - p_o$ and $\rho' = \rho - \rho_o$

Using equation (4), the equations (1) to (4) were linearized and expressed in the matrix form neglecting the viscosity.

$$\begin{vmatrix} (-iK_x gH) & 0 & 0 & (i\omega) \\ (-iK_z gH - g) & (g) & (i\omega) & 0 \\ (i\omega) & (-i\omega\gamma) & (\frac{\gamma-1}{H}) & 0 \\ 0 & (i\omega) & -(\frac{1}{H} + iK_z) & (-iK_x) \end{vmatrix} \begin{vmatrix} p' \\ \rho' \\ \omega \\ u \end{vmatrix} = 0 \qquad (5)$$

For a non trivial solution of this system to exist, the determinant of the coefficient matrix must vanish. This condition yields the dispersion relation (Hines, 1960).

$$\omega^4 - \omega^2 a^2 (K_x^2 + K_z^2) + (\gamma-1)g^2 K_x^2 + i\omega^2 \gamma g K_z = 0 \qquad (6)$$

The dispersion relation is fourth order in $\omega$, indicating the possibility of four separate solutions to the system. The solutions may be identified as two acoustic and two gravity waves. The two solutions of each type do not represent waves with different characteristics, but merely

23

two waves whose phases propagate in opposite directions.

Examination of (6) shows that a wave amplitude variation must occur in either the vertical or horizontal direction. We assume that $K_x$ is purely real, which means that no attenuation of waves occurs in the horizontal direction. Examining the imaginary part of equation (6) we see that (Hines 1960)

$$\omega^2 a^2 (2\mathrm{Re}K_z \mathrm{Im}K_z) = \gamma g \omega^2 \mathrm{Re}K_z \tag{7}$$

so that either

$$\mathrm{Re}\ K_z \equiv 0 \quad (K_z \text{ imaginary}) \tag{8}$$

$$\mathrm{Im}\ K_z = \gamma g / 2a^2 \tag{9}$$

The first alternative means that the waves have no vertical phase variation, but only an exponential decay (or amplification) with height. This is the characteristic of a "surface" or boundary wave. The second alternative allows real phase propagation both vertically and horizontally and defining:

$$k_z \equiv \mathrm{Re}K_z \tag{10}$$

$$k_\chi = \mathrm{Re}K_x \tag{11}$$

so

$$K_z = k_z + \frac{i\gamma g}{2a^2} \tag{12}$$

The Brunt frequency for an isothermal atmosphere is given by

$$\omega_B{}^2 = (\gamma - 1)\frac{g^2}{a^2} \tag{13}$$

24

and define the acoustic cutoff frequency (Hines 1960)

$$\omega_a = \frac{\gamma g}{2a} = \frac{a}{2H} \tag{14}$$

the dispersion relation can be written in the form
(Pitteway and Hines 1965)

$$N_z^2 = (1 - \frac{\omega_a^2}{\omega^2}) - N_x^2(1 - \frac{\omega_B^2}{\omega^2}) \tag{15}$$

where $N_x = \frac{ak_n}{\omega}$ and $N_z = \frac{ak_z}{\omega}$. This is identical to the
form given by Tolstoy (1963)

$$\gamma^2 = \frac{\omega^2}{a^2} - \alpha^2 + \frac{\alpha^2}{\omega^2}N^2 - \nu^2 \tag{16}$$

where his notation is related to Hines (1960) by

$$N = \omega$$

$$\gamma = k_z$$

$$\alpha = k_n$$

$$\nu = \omega_{a/a} = \frac{\gamma g}{2a^2} = \omega_{a/a}$$

From the dispersion relation (16) and the definition s of
the phase and group velocities, Georges (1967) obtained

$$Vp = \omega/k$$

$$Vg = \partial\omega/\partial k$$

Some useful relations for certain simplified and limiting
cases. The horizontal phase and group velocities are:

$$V_{px} = \left[ \frac{\omega^2 - \omega_B^2}{\omega^2/a^2 - k_z^2 - \nu^2} \right]^{\frac{1}{2}} \tag{17}$$

$$V_{gx} = \frac{(k_z^2 + \nu^2 - \omega^2/a^2)^{\frac{1}{2}}(\frac{\omega_B^2}{\omega^2} - 1)^{3/2}}{\frac{\omega_B^2}{\omega^3}(k_z^2 + \nu^2 - 2\frac{\omega^2}{a^2}) + \frac{\omega^2}{a^2}}$$

25

where $\nu = \frac{1}{2}\pi$

Both the phase and group velocities approach the sound speed in the high-frequency limit for acoustic waves.

Considerable work on atmospheric wave propagation studies was done to explain the nuclear bomb effects. Pfeffer and Zarichny (1963) and Harkrider (1964) calculated theoretical microbarograms and compared them with experimental data. They examined the variations of the dispersion curve structure due to changes in the atmospheric model assumed and identified various modes as acoustic and gravity by their behavior as the frequency becomes large. The general properties of such atmospheric waves were applied to upper atmospheric phenomena such as TIDs, by Hines (1960). Hines (1960) showed that the wave energy was strongly reflected at levels somewhat below TID occurrence heights and was strongly ducted. The duct was subject to some leakage upward into F region. The horizontal propagation could then occur with little attenuation, primarily within the slightly leaky duct, but enough energy could escape upward to provide a TID propagation.

If one assumes that the speeds, sizes and wave front tilts of TIDs are similar to free internal gravity waves, then the properties of such waves may be determined from the properties of the thermosphere. The limiting value of

wave front tilt with the vertical for an isothermal atmosphere
is given by the theory (Tolstoy 1963)

$$\cos \theta = \tau_B/\tau$$

where $\tau_B$ is the Brunt period. If we take the Brunt period
$\tau_B = 14$ minutes for F region levels using 1962 U.S. Standard
atmosphere, then for wave periods of 20 minutes, the tilt
would be $64^\circ$. The wave front tilts in all the 18 sample
TIDs were computed by taking $\tau_B$ as 14 and 10.5 minutes and
the computed values are presented in table 2 to compare with
the experimentally observed values. This means that the
neutral atmosphere should be much cooler than the U. S.
Standard atmosphere. These calculations seem to indicate
that long period TIDs may be due to free internal gravity
waves but more data is necessary to substantiate this
conclusion.

The other alternative is to interpret TID as imperfectly
ducted gravity waves. Friedman (1966) considered the poss-
ibility of internal gravity waves in leaky ducts to explain
TID observations. His calculations showed that, for a given
mode, the phase and group velocities are nearly equal and
relatively constant with the period with the maximum horizon-
tal velocity of 300 m.sec$^{-1}$. The observed speeds of TIDs
and the apparent direction of TIDs arriving from winter
polar regions appear to agree with Friedman's calculations

of wave characteristics. It is also observed that the winter mesosphere heatings are frequent which would effect the mesospheric temperature decline (Maeda and Young 1966). These mesospheric warmings cause leaky duct conditions for the gravity wave energy to leak upwards to produce TIDs in the F region.

The observed seasonal variation in the TID directions (i.e. TIDs travelling away from the winter pole) may be accounted for to some extent as due to leaky duct conditions being present in winter polar mesosphere levels. The temperature profiles of Champion (1957) do indicate an appreciable weakening of the winter duct around 80 km, compared to summer conditions for middle latitudes.

8. <u>Long period soundwaves generated by Saturn-Apollo launches</u>

Wave like disturbances were observed in the ionosphere following several nuclear explosions in early 1960s. Baker (1968) detected the disturbance at 150-200 km altitude with periods of one minute and speeds 300 m.sec$^{-1}$. The periods and propagation characteristics of the ionospheric disturbances were essentially the same as those observed on the ground. Baker (1968) interpreted these ionospheric disturbances as manifestations of imperfectly ducted acoustic gravity waves. Acoustic signals which can propagate long

distances (or the order of a thousand kilometers) from
large rockets were also detected and reported by Donn et
al (1968, 1971).

Ionospheric variations due to Saturn-Apollo launches
were noticed from the ionograms taken at Wallops Islands,
Va., and Grand Bahama Islands (Fehr, 1968). Disturbances
on Grand Bahama ionograms were observed for a period of
almost two hours. A small kink on the ionogram appeared
which travelled downward. The disturbances also created
several additional stratifications (traces) on the ionograms.
Disturbances such as these were also observed by Golomb
(1963) during chemical release experiments.

A CW doppler array was in operation at Westwood, N.J.
during the launchings of Saturn-Apollo 12 and 13 rockets.
These launches produced long period sound waves which were
successfully detected by the doppler array soundings
(Tolstoy et al 1970). Figure 13 shows the raw CW doppler
data for Saturn-Apollo 12 launch on Nov. 14, 1969. The oper-
ating frequencies were 4.8 and 6.03 MHz. The CW doppler
data for Lebanon and Thornhurst immediately before the signal
arrival between the time window 1100 to 1220 EST was subject-
ed to cross spectral analysis to study the background noise
coherence. It can be seen from the figure 14 that the
background noise coherence is rather poor in entire period

29

band and remained less than 0.2. Cross spectral analysis
between several station pairs during the time of signal
interval 1220-1340 was adopted to find the dominant periods.
The results of the cross spectral analysis are presented
in figures 15, 16 and 17. It can be seen from the figures
that at the time interval including the signal there is
a concentration of energy in the period band 1 to 5 minutes.
The CW doppler data was then filtered using a bandpass
filter of 1 to 5.02 minutes and the resulting plot is
presented in figure 18. Normal acousitic signals of 330m/s
arrive at 1222 hours. Earlier arrivals at 1208 propagated
with group velocities of about 450 m/s.

Ionograms taken every 60 seconds on the day of Saturn-
Apollo 12 launch from Wallops Island, Va., were examined
to detect any disturbances caused by the Saturn rocket. It
was found that a kink on the ionogram near the ordinary F2
layer critical frequency existed which slowly moved
downward before merging to F2 layer ordinary ray trace.
Several additional stratifications were noticed all over the
F2 region indicating the disturbed nature of the ionosphere.
The ionograms were then subjected to true height analysis
to study the electron density fluctuations due to the Saturn
rocket. Electron density variations at various heights
were plotted against local time and the plot is shown in

figure 19. It can be seen from figure 19 that the undulations in electron density at various heights has a period of 2-3 minutes. It might be of interest to note that the maximum effect on the ionosphere by the rocket was felt around 1218. If the distance between Wallops Islands and ground range of rocket when in F2 region was taken approximately as 1000 km, then the group velocity of the arrival of the signal to ionospheric levels over Wallops Islands was of the order of 450 m.sec$^{-1}$.

The CW doppler array data was subjected to cross correlation analysis to compute the phase speeds and directions. Results of the analysis are presented in Table 3. The average phase velocity was found to be 700-800 m.sec$^{-1}$ coming from south of the array. The variations in the phase velocities during the signal may be due to the nature of the source, which is a supersonic disturbance moving in both horizontal and vertical dimensions. Also, there are some inherent experimental errors due to the height changes introduced due to the obliquity of received radio waves.

Of particular interest, are the group velocities of the order 450 m.sec$^{-1}$ obtained for the earliest visible disturbances seen on the doppler records from Westwood, N.J. and ionograms from Wallops Island, corresponding to periods

# TABLE 3

## Phase Velocities of the Saturn-Apollo 12 Signal

## As Seen on Westwood, N.J. Doppler Array

| Time | Velocity (m.sec$^{-1}$) | Direction (Degrees) |
|---|---|---|
| 1225-1235 | 810 | 185 |
| 1238-1248 | 808 | 178 |
| 1251-1301 | 750 | 176 |
| 1304-1314 | 700 | 177 |
| 1317-1327 | 650 | 140 |

in the range 2-4 minute and horizontal phase velocities near 800 m.sec$^{-1}$, Tolstoy et al (1971) tried to explain (from CW doppler signal variations) these arrivals of signals in terms of waveguide effect in which sound is totally reflected from the thermosphere by the bending back of rays, and sound is totally (or almost totally) reflected from the underlying mesosphere because of stronger density gradients and the consequent increase in the acoustic cutoff frequency. Thus sound would be channeled at the ionospheric heights near the bottom of the thermosphere.

9. Ionospheric Irregularities and Internal Atmospheric Gravity Waves:

Hines (1960) put forward rather strong arguments to explain some of the ionospheric phenomena as manifestation of internal atmospheric gravity waves. We discuss here the apparent correlation between TIDs and sporadic E using gravity wave concepts.

Martyn (1959) tried to explain the formation of some types of Es at low and middle latitudes by ionization inhomogeneities moving downward. Experimental data from ionosondes show that there exists some relationship between F and E regions of the ionosphere, (Fejer, 1959, Bowman 1959). Ovezgel'dyyev and Korsunova (1964) and Ovezgel'dyyev and Vasil'yeva (1964) showed on the basis of data obtained in

33

1962, that in some cases the $F_O$ layer observed in the F-region, gradually changed into sporadic E layer. Generally it took 1 to 3 hours for the secondary formation, which gradually changed into an Es. It was also shown that the transformation of a secondary formation in the F region into an Es was apparently independent of magnetic activity. The data also indicated that the process of transformation depended on the time of the day and season and to some extent on the solar activity level. Castel and Faynot (1964) observed from a study of ionograms that irregularities first appear in the F region and move downward, producing weak sporadic E. Recently Ryss et al. (1969) studied the variation of electron concentration during travelling ionospheric disturbances. During the passage of TIDs, electron density at fixed levels was subjected to quase-periodic variations and the period of oscillation depended on the fixed level. The period tends to increase with increasing height: the average period is 20 to 40 min at heights of 120-150 km, and 50-60 min at heights of 150-200 km. Short period oscillations (2-5 min) are superposed on the main oscillation with relatively long periods (20-50 min). Ryse et al (1969) used N(h) profiles obtained for one minute iono-grams to compute the rates of appearance of the same phase of quasi-periodic oscillations at different fixed levels, which

were in the order of 100 m.sec$^{-1}$. Simultaneous analysis of
N(h) profiles and corresponding ionograms showed that in many
cases the appearance of a sporadic E layer is associated
with TIDs. This occurs most frequently when developing TID
is accompanied by a change in electron concentration at all
ionospheric levels, including the E region.

Sharadze and Kvavadze (1967) pointed out that if an Es
layer already exists at the time of passage of TIDs, then
they sometimes produced an increase in $f_oE_s$ by a factor of
15-20. We have investigated the occurrence (or increase)
of sporadic E ionization at times in which medium scale
TIDs are observed on the CW doppler records. Published
ionogram data from Bellarica, Massachusetts (42.5$^o$N, 71.2$^o$W,
approximately the same latitude as our Catskill station)
during the TID events were examined for possible clues on
the occurrence of sporadic E. We have noticed that in about
60% of the cases during the winter of 1969-70, the sporadic
E either appeared or increased (i.e. increase in $f_bEs$ value)
after 20-120 minutes of the passage of a TID. This result strong-
ly suggests some apparent connection between the passage of a
TID and occurrence of sporadic E ionization. The significance
of this result may be explained to some extent using internal
atmospheric gravity wave concepts.

Chernysheva et al (1970) examined sixty six cases of TIDs and reported that if a TID disturbance embraces the ionospheric E region as it develops, then an Es burst was observed in 50% of the cases, generally 15-20 minutes after the appearance of the disturbance. In some cases the duration and appearance of Es burst reached 30-40 minutes after the appearance of the TID. The magnitude of the Es varied between 0.5 to 5 MHz and depended on the intensity of the TID.

Hines (1968) argued that if the case for a gravity wave interpretation for TIDs is accepted, then it is natural to extrapolate the interpretation downward: the waves are believed to be propagating upwards to the F region levels producing TIDs. In their way up the waves travel through the region of Es occurrence. Also the wave spectrum must be broader at the lower levels since dissipation is less severe there. The combined effect of filtering action of dissipative forces and windshears probably can account to some extent for the apparent correlation between TIDs and sporadic E ionization. Recently Chimonas (1971) examined the theory of enhancement of sporadic E by horizontal transport within the layer. The tidal winds in the E region acting through wind shear mechanism produce thin horizontal layers of metallic ions. These metallic ions descend in time as the

phase of the wind change. Gravity waves generated below E region
have a downward phase velocity and if this is the same order
of magnitude of the descent velocity of the layer, the wave seen
by the ions in the layer can be almost stationary in time.
The interaction of the wave with the layer then produces a
very strong horizontal redistribution of the ion density.
This process may be responsible for producing patches of Es
ionization. The sporadic nature of the layer may be due to
the presence of variability of suitable waves while the
horizontal scale of the sporadic ionization clouds may be
controlled by the horizontal wave lengths of the gravity
waves.

Our investigation clearly supports the gravity wave
interpretation for the relation of sporadic E and TIDs.
The TID wave front tilts and speeds reported in our
investigation are in reasonable limits to account for TID
passage and sporadic E ionization appearance (or increase)
using internal atmospheric gravity wave concepts.


3. Conclusions:

CW doppler data collected from northern hemisphere
middle latitude stations has been analyzed to investigate
travelling ionospheric disturbances and the dynamics of
the upper atmosphere. The following are the main conclusions

drawn from this study.

1. During summer and winter seasons in both hemispheres, the TIDs travel away from the winter polar regions.

2. During fall and spring seasons, disturbances in the northern hemisphere travel approximately westward, while those in the southern hemisphere travel eastward.

3. The propagation parameters of the observed disturbances such as the phase speeds, wavelengths and periods are in general similar to the parameters of acoustic gravity waves and hence it may be concluded that the TIDs are manifestations of atmospheric gravity waves propagating in the upper atmosphere.

4. The observed characteristics of the medium scale TIDs fit rather well with Friedman's theory of 'leaky' duct propagation with regard to size and speed.

5. The observed seasonal variations of TID directions may be explained to some extent by the seasonal variation in the mesospheric temperature. The mesospheric temperature inversion does not totally disappear in winter but the temperature profiles of Champion (1957) indicate an appreciable weakening of winter duct around 80 km relative to the summer conditions, especially at middle latitudes. Also some support to

this conclusion is found in observations of mesospheric heating in winter polar region (Maeda and Young 1966), since gravity wave energy penetrates upwards much more easily in the mesospheric temperature decline. The effect of this seasonal variation in mesospheric temperature would be that the acoustic gravity wave energy in summer might be transported over large horizontal distances due to almost perfect duct, while, in winter, would be lost to the thermosphere by leak ducts and by oblique upward propagation.

6. Study of ionograms showed that the ionospheric irregularities first appeared in the upper F-region and moved downward producing weak sporadic E ionization. Results of the present study showed an apparent connection between the passage of TIDs and appearance of sporadic E ionization. This apparent connection between TIDs and sporadic E can not be satisfactorily explained using hydromagnetic wave theory since hydromagnetic waves travel much faster than the observed disturbance. However, this result can be explained to some extent using the atmospheric gravity wave concepts. The interaction of the gravity waves (whose phase propagation downwards is of the same order of magnitude of metallic ion layers

which are formed due to tidal E region winds through wind shear mechanism) with the descending metallic ion layers may produce a strong horizontal redistribution of the ion density which may be responsible for the formation patchy ionization.

Beynon, W.J.G., Evidence of horizontal motion in F2 region
    ionization.  Nature 162, 887, 1948.

Beynon, W.J.G. and L. Thomas, Travelling disturbances in F2
    region and magnetic activity.  'Rocket exploration of the
    upper atmosphere', ed. R.L.F. Boyd; 1954.

Blackman, R.B., and J.W. Tukey, "The measurement of Power
    Spectra", Dover Publications, New York

Bowman, G.G., Travelling disturbances associated with ionospheric
    storms", J. Atmosph. Terrest. Phys., 27, 1247, 1965.

Bowman, G.G., Movements of ionospheric irregularities and
    gravity waves, J. Atmosph. Terrest. Phys., 30, 721, 1968.

Bramley, E.N., Direction finding studies of large scale iono-
    spheric irregularities.  Proc. Roy. Soc. London 220, 39,
    1953.

Bramley, E.N. and W.J. Ross, Measurements of direction arrival
    of short radiowaves reflected at the ionosphere.  Proc.
    Roy. Soc. London 207, 252, 1951.

Castel, F. du, and J.M. Faynot, Some irregularities observed
    simultaneously in the upper and lower ionosphere at middle
    latitudes.  Nature 204, 986, 1964.

Chan, K.L. and O.G. Villard, Jr., Observation of large scale
    travelling ionospheric disturbances by spaced-path high
    frequency instantaneous frequency measurements.  J. Geophys.
    Res. 67, 973, 1962.

Chang, N.F., Acoustic gravity waves in the ionosphere and their
    effects on high frequency radio propagation.  Ph. D. Thesis
    Univ. of Colorado, 1968.

Chernysheva, S.P., V.M. Sheftel', and A.M. Mozhayer, Relation-
    ship between travelling ionospheric disturbances and Es.
    Geomag. and Aeronomy, 10, 872, 1970

Chimonos, G., Enhancement of Es by horizontal transport within
    the layer., J. Geophys. Res., 76, 4578, 1971.

Davies, K., Doppler studies of the ionosphere with vertical
    incidence., Proc. IRE 50, 94, and correction on 1544, 1962.

Davies, K. and D. Baker, F2-region acoustic waves from severe weather., J. Atmosph. Terr. Phys. 31, 1345, 1969.

Davies, K. and J.L. Jones, Three dimensional observations of travelling ionospheric disturbances., J. Atmosph. Terr. Phys., in press, 1971.

Donn, W.L., E. Posmentier, U. Fehr and N.K. Balachandran, Infrasound at long range from Saturn V, Science.

Donn, W.L., D. Cotten, Sound from Apollo Rockets in Space, Science, 171, pp. 565-567.

Fehr, U., Propagating energy in the upper atmosphere including lower ionosphere generated by artificial sources., Proc. of the ESSA/ARPA Acoustic-Gravity Wave Symp. 87, 1968.

Fejer, J.A., Hydromagnetic wave propagation in the ionosphere. J. Atmosph. Terr. Phys. 18, 135, 1960.

Friedman, J.P., Propagation of internal gravity waves in a thermally stratified atmosphere. J. Geophys. Res. 71, 1033, 1966.

Georges, T.M., Ionospheric effects of atmospheric waves. IER 57 - ITSA 54. 1967.

Georges, T.M., HF doppler studies of travelling ionospheric disturbances, J. Atmosph. Terr. Phys. 30, 735, 1968.

Golomb, D., N.W. Rosenberg, J.W. Wright, R.W. Barnes., Formation of electron depleted region in the ionosphere by chemical releases., Space Research IV., North-Holland Pub. Co., 1964.

Goodwin, G.L., Some horizontally-moving ionospheric irregularities at high latitudes, Planetary and Space Science, 16, 273, 1968.

Harkrider, D.G., Theoretical and Observed acoustic gravity waves from explosive sources in the atmosphere, J. Geophys. Res., 69, 5295, 1964

Heisler, L.H., Anomalies in ionosonde records due to travelling ionospheric disturbance. Aust. J. Phys. 11, 79, 1958.

Hines, C.O., Internal atmospheric gravity waves at ionospheric heights., Cand. J. Phys. 38, 1441, 1960.

Hines, C.O., Application of gravity wave theory to upper atmospheric studies. "Winds and Turbulence in Stratosphere, Mesosphere and Ionosphere". North-Holland Publishing Co., 1968.

Hooke, W.H., Ionospheric irregularities produced by internal atmospheric gravity waves. J. Atmosph. Terr. Phys. 30, 795, 1968.

Hunsucker, R.D. and L.H. Tveten, Large travelling ionospheric disturbances observed at middle latitudes utilizing the high resolution H.F. backscatter technique, J. Atmosph. Terr. Phys. 29, 909, 1967

Jones, J.E., Observation of travelling ionospheric disturbances by the doppler technique with spaced transmitters. ESSA – Tech Report ERL 142 – SDL – 11, 1969.

King, G.A.M., The ionospheric disturbances and atmospheric waves., J. Atmosph. Terr. Phys., 28, 957, 1966.

Lamb, H., On the theory of waves propagated vertically in the atmosphere, Proc. Lond. Math. Soc. 1, 122, 1909.

Liszka, L., and G.N. Taylor, A synoptic study of large scale ionospheric irregularities using observations of Faraday rotation of satellite signals. J. Atmosph. Terr. Phys. 27, 843, 1965.

Martyn, D. F., Cellular atmospheric waves in the ionosphere and troposphere. Proc. Roy. Soc. A201, 216, 1950.

Martyn, D.F., Sporadic E ionization, Spread F and twinkling of radio stars., Nature, 183, 1382, 1959.

Maeda, K. and J.M. Young, Propagation of pressure waves produced by auroras. J. Geomag. Geoelec. 18, 275, 1966.

Montes, H.A., C. Grosch, E. Posmentier and M. Hinich, Summary report on atmospheric propagation studies. No. IWL-7556-175. Teledyne Isotopes, Westwood, N. J. July 1970.

Munro, G.H., Travelling disturbances in the ionosphere. Proc. Roy. Soc. 202, 208, 1950.

Munro, G.H., Reflections from irregularities in the ionosphere, Proc. Roy. Soc. A219, 447, 1953a.

Munro, G.H., Travelling disturbances in the ionosphere. Changes in diurnal variation. Nature 180, 1252, 1953b.

Munro, G.H., Travelling ionospheric disturbances in the F region of the ionosphere. Aust. J. Phys. 11, 91-92, 1958.

Osborne, D.G., Horizontal movements of ionization in the equatorial F. region. J. Atmosph. Terr. Phys. 6, 117, 1955.

Ovezgel'dyyev, O., and l.P. Korsunova, The sporadic E layer of the ionosphere and daily variations of the earth's magnetic field. Geomag. & Aeronomy SSSR, 2, 322, 1964.

Ovezgel'dyyev, O., and A.V. Lezhneva, Relationship between Es and F region of the ionosphere. Geomag. & Aeronomy, SSSR, 6, 873, 1965.

Ovezgel'dyyev, O. and Ye. K. Vasil'yeva, On the theory of the formation of Es in middle latitudes. Geomag. & Aeronomy, SSSR, 2, 321, 1964.

Pfeffer, R.L. and J. Zarichny, Acoustic gravity wave propagation in an atmosphere with two sound channels., Geofis. Purs, Appl. 55, 175, 1963

Price, R.E., Travelling disturbances in the ionosphere. Nature 172, 115, 1953.

Price, R.E., Travelling disturbances in the ionosphere. Physics of the Ionosphere. Phys. Soc. 181, 1955

Pierce, J.A. and H.R. Mimno, The reception of radio echoes from distant ionospheric irregularities. Phys. Rev. 57, 95, 1940.

Ryss, I.K., S.P. Chernysheva, Z.S. sharadze and V.M. Shefter, Variations in electron concentrations during vertically travelling disturbances., Geomag. and Aeronomy, 9, 896, 1969.

Sharadze, Z.S. and D.K. Kavadze,

Geomag. and Aeronomy, 6, 773, 1966.

Skinner, N.J., R.A. Brown, and R.W. Wright, Multiple stratification of the F-layer at Ibadan. J. Atmosph. Terr. Phys. 5, 92, 1954.

Sen, H.Y., Stratification of the F2 layer of the ionosphere over Singapore., J. Geophys. Res. 54, 363, 1949.

Titheridge, J.E., Periodic disturbances in the ionosphere, J. Geophys. Res. 73, 243, 1968.

Thomas, L., Some measurements of horizontal movements in F2 region using widely spaced observing stations. J. Atmosph. Terr. Phys. 14, 123, 1959.

Thome, G.D., Incoherent scatter observations of travelling ionospheric disturbance. J. Geophys. Res. 69, 4047, 1964.

Thome, G. and P.B. Rao, Comparison of acoustic gravity wave theory with HP and UHF observations. ARPA Report. Contract DA-01-021-14482(Z), 1969.

Tolstoy, I., The theory of waves in stratified fluids including the effects of gravity and rotation. Rev. Mod. Phys. 35, 207, 1963.

Tolstoy, I., H. Montes, G. Rao and E. Willis, Long Period sound waves in the thermosphere from Apollo launches. J. Geophys. Res. 75, 5621, 1970.

Wells, H.W., J.M. Watts, and D.E. Georges, Detection of rapidly moving ionospheric clouds. Phys. Rev. 69, 540, 1946.

Wilson, C.R., Infrasonic pressure waves from the aurora, a shock wave model, Nature, 216, 131, 1967.

Wright, J.W., Ionosonde studies of some chemical releases in the ionosphere, Radio Science J. of Res., NBS, 68D, 1964.
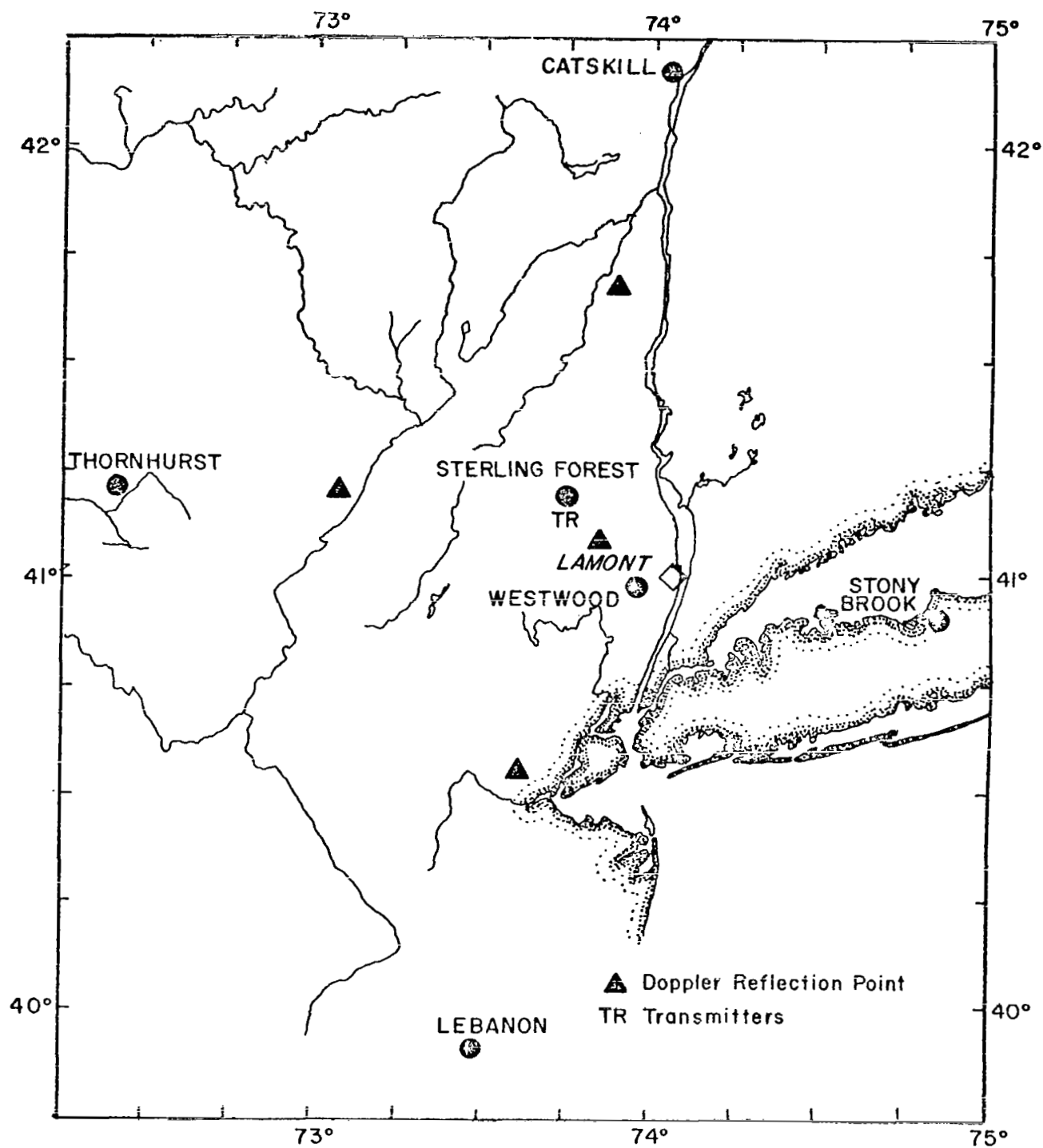
Figure 1: Geographic location of the stations of the CW doppler array.
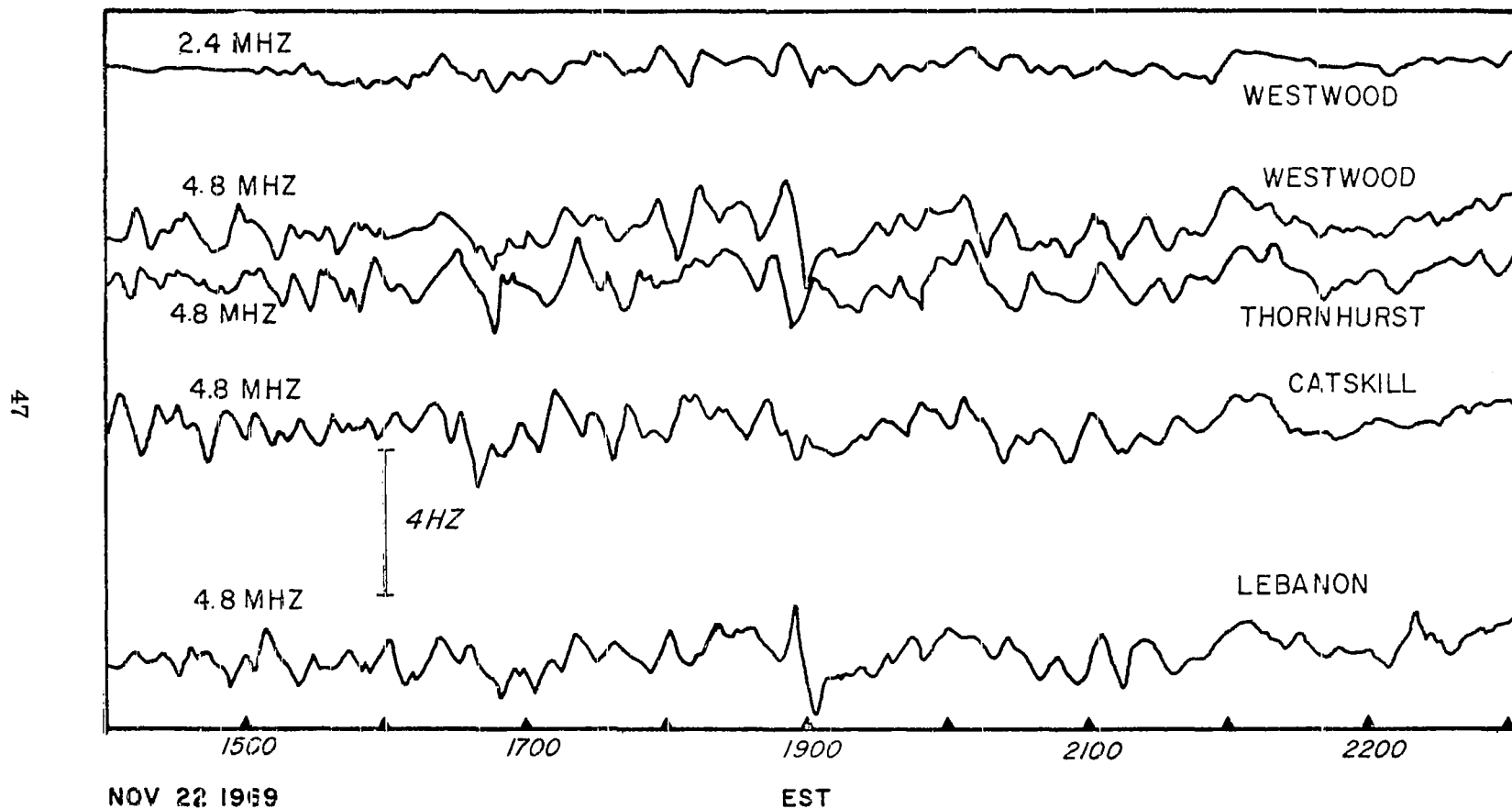
Figure 2: Typical TID seen on a CW doppler record.
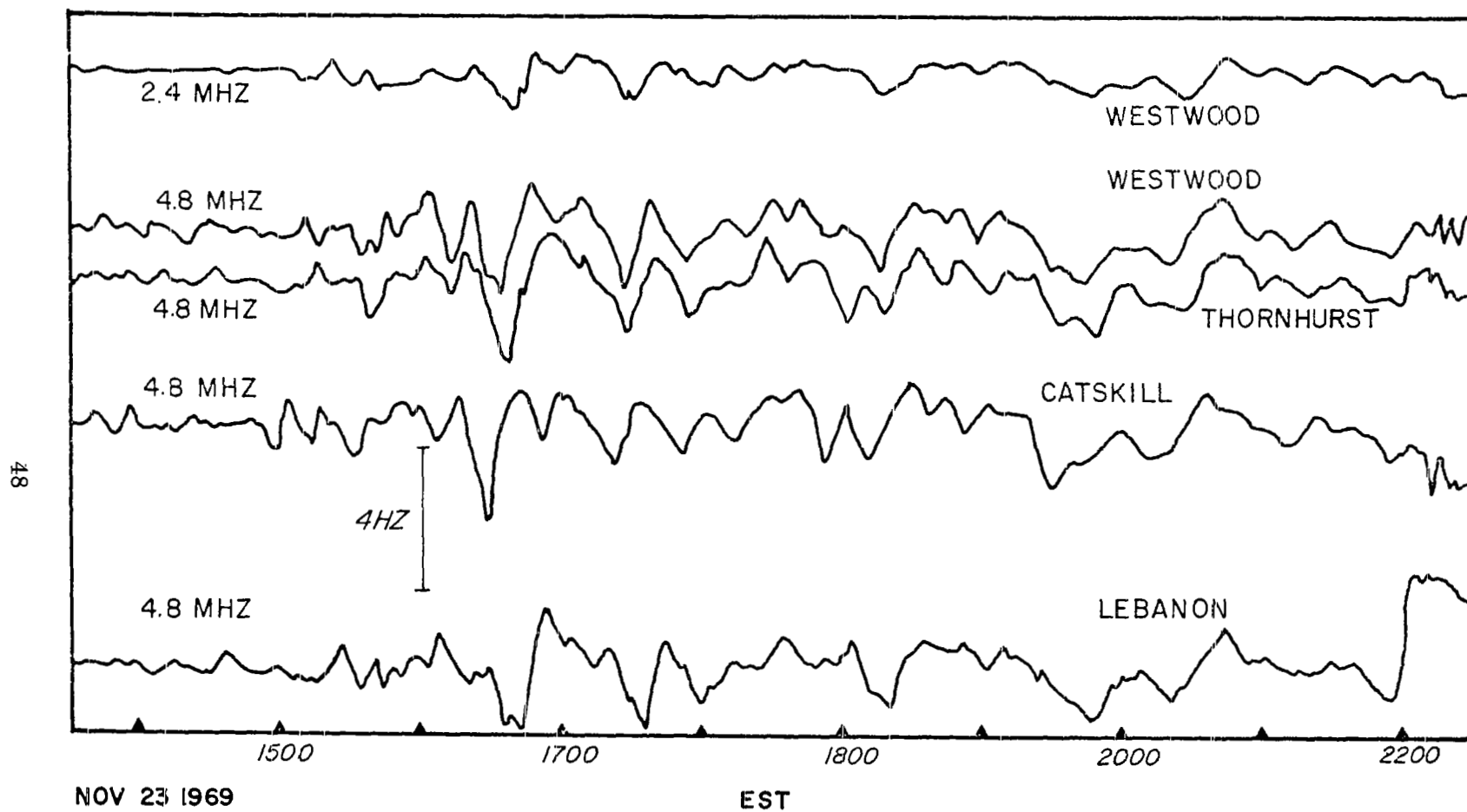
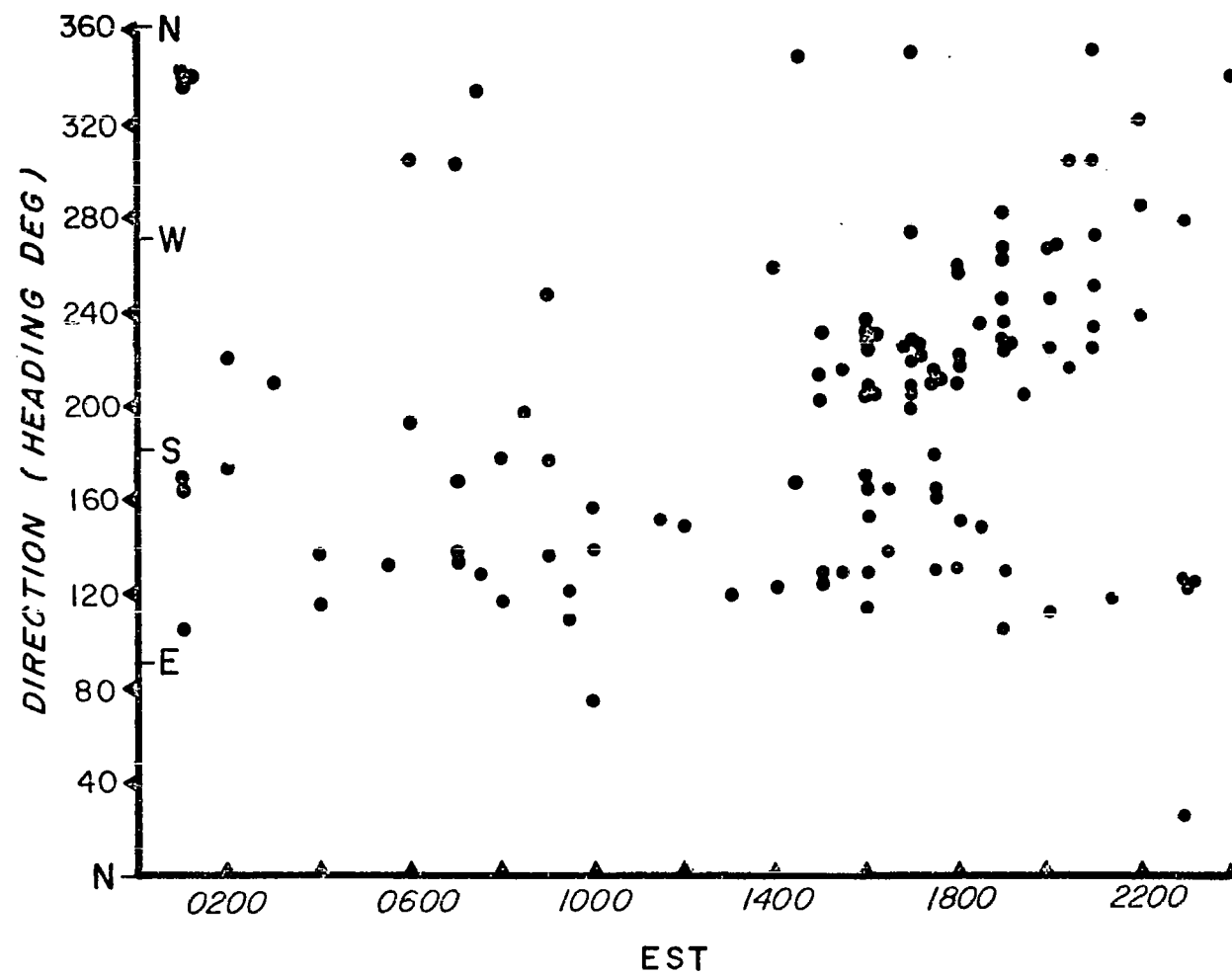Figure 3: Typical TID seen on a CW doppler record.
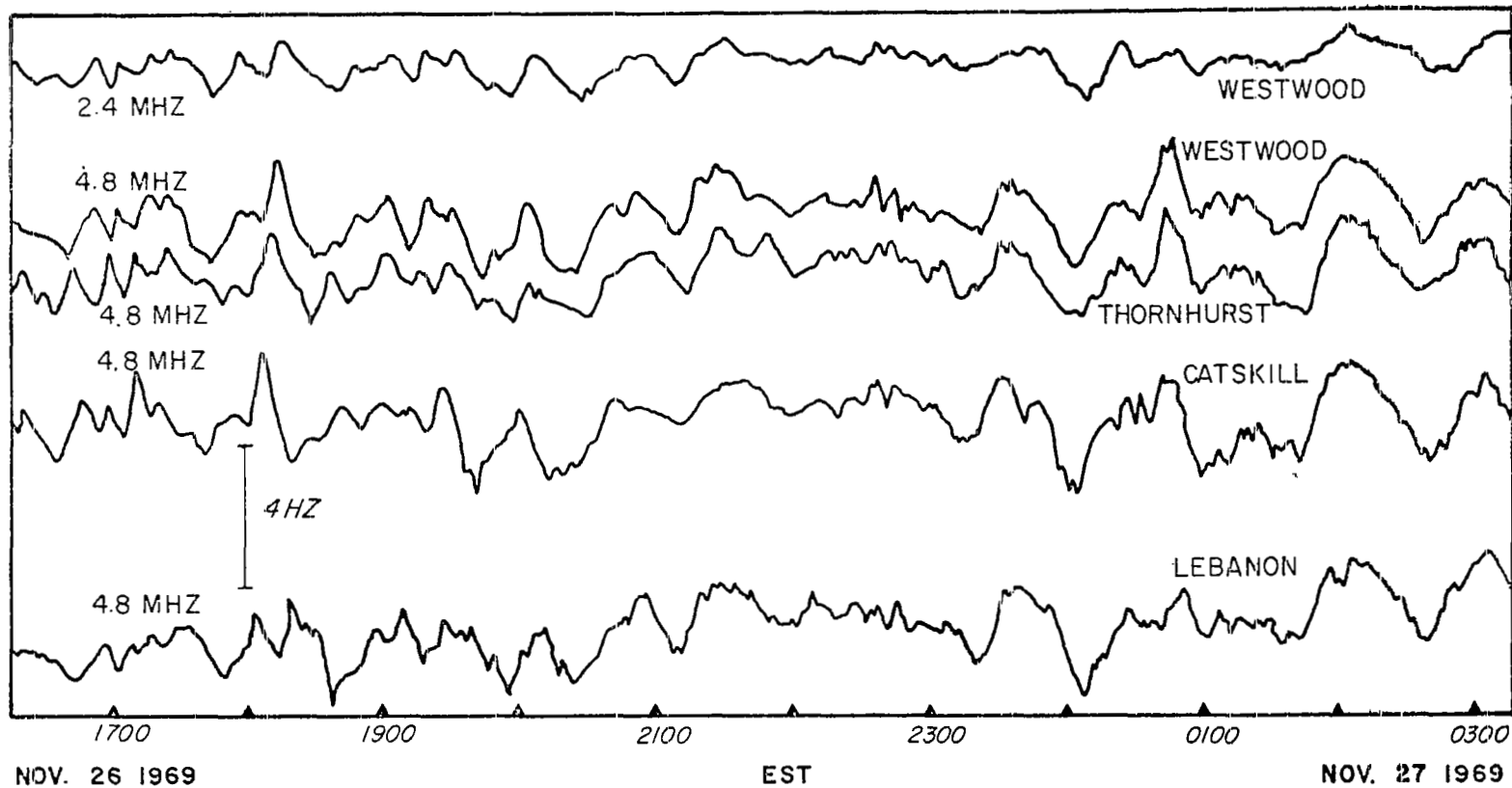
Figure 4: Typical TID seen on a CW doppler record.

WESTWOOD

4 HZ

CATSKILL

LEBANON

50

30 NOV 1969

1600    1700    1800    1900    2000    2100    2200    2300

EST
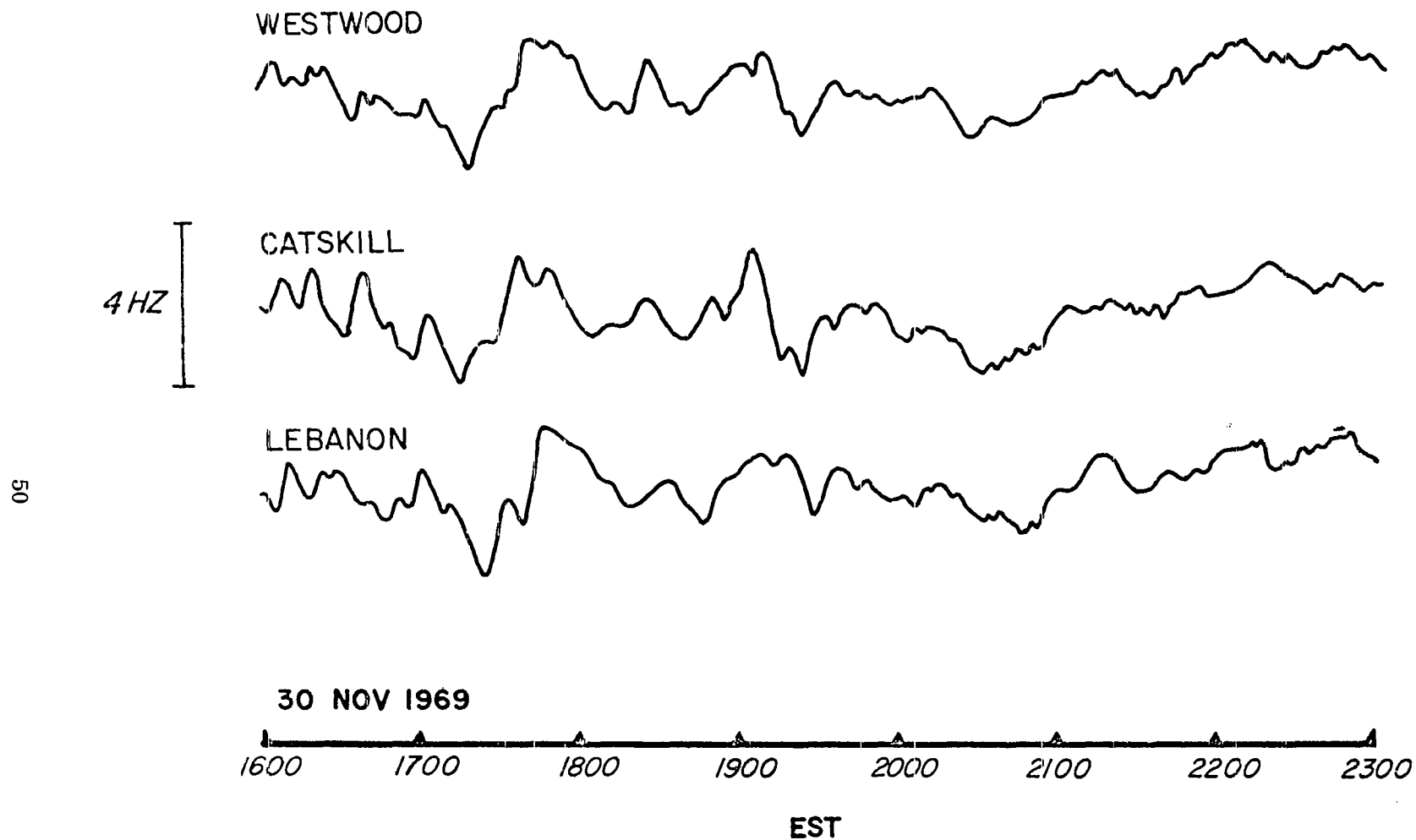
Figure 5:  Typical TID seen on a CW doppler record.
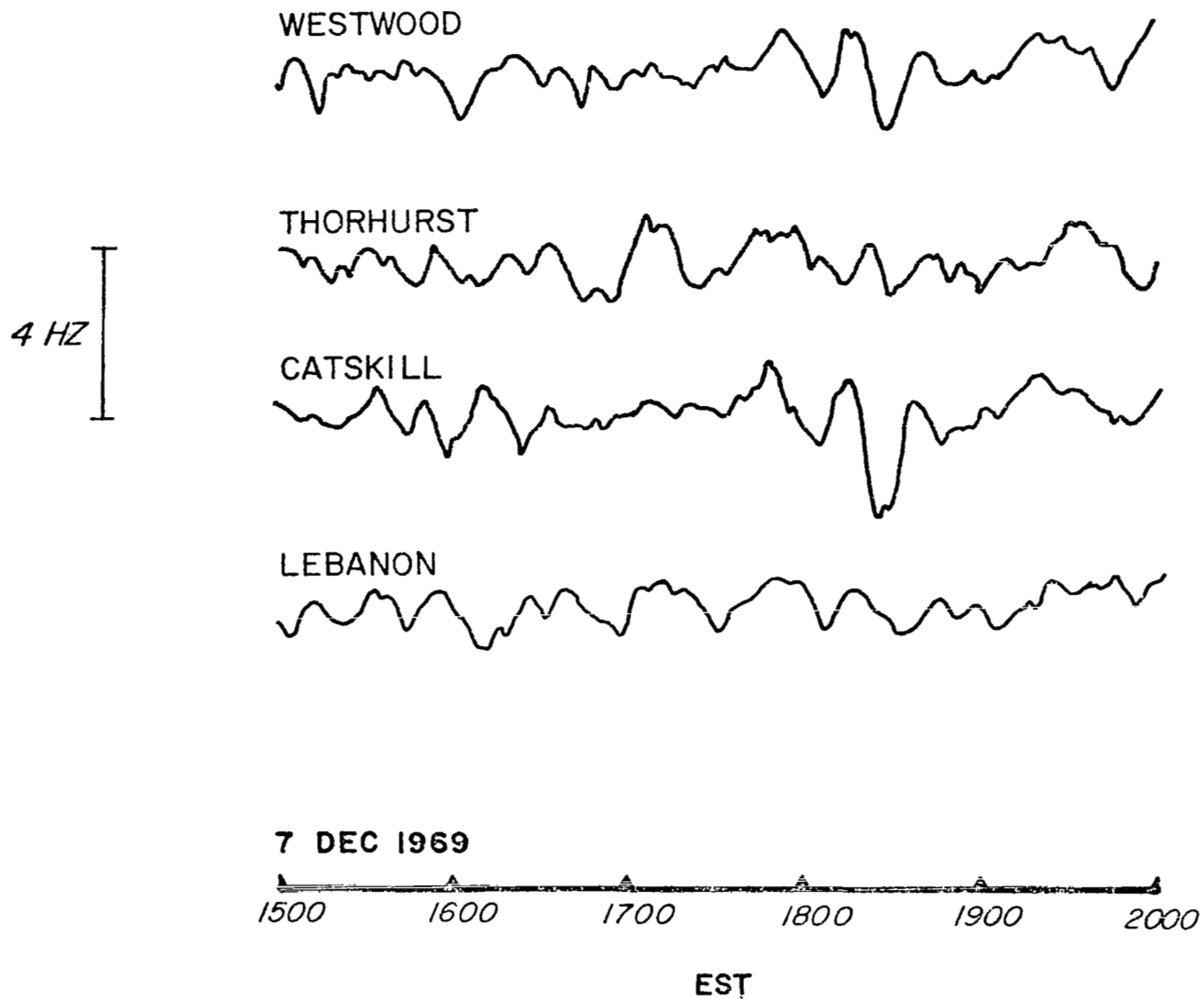
Figure 6: Typical TID seen on a CW doppler record.
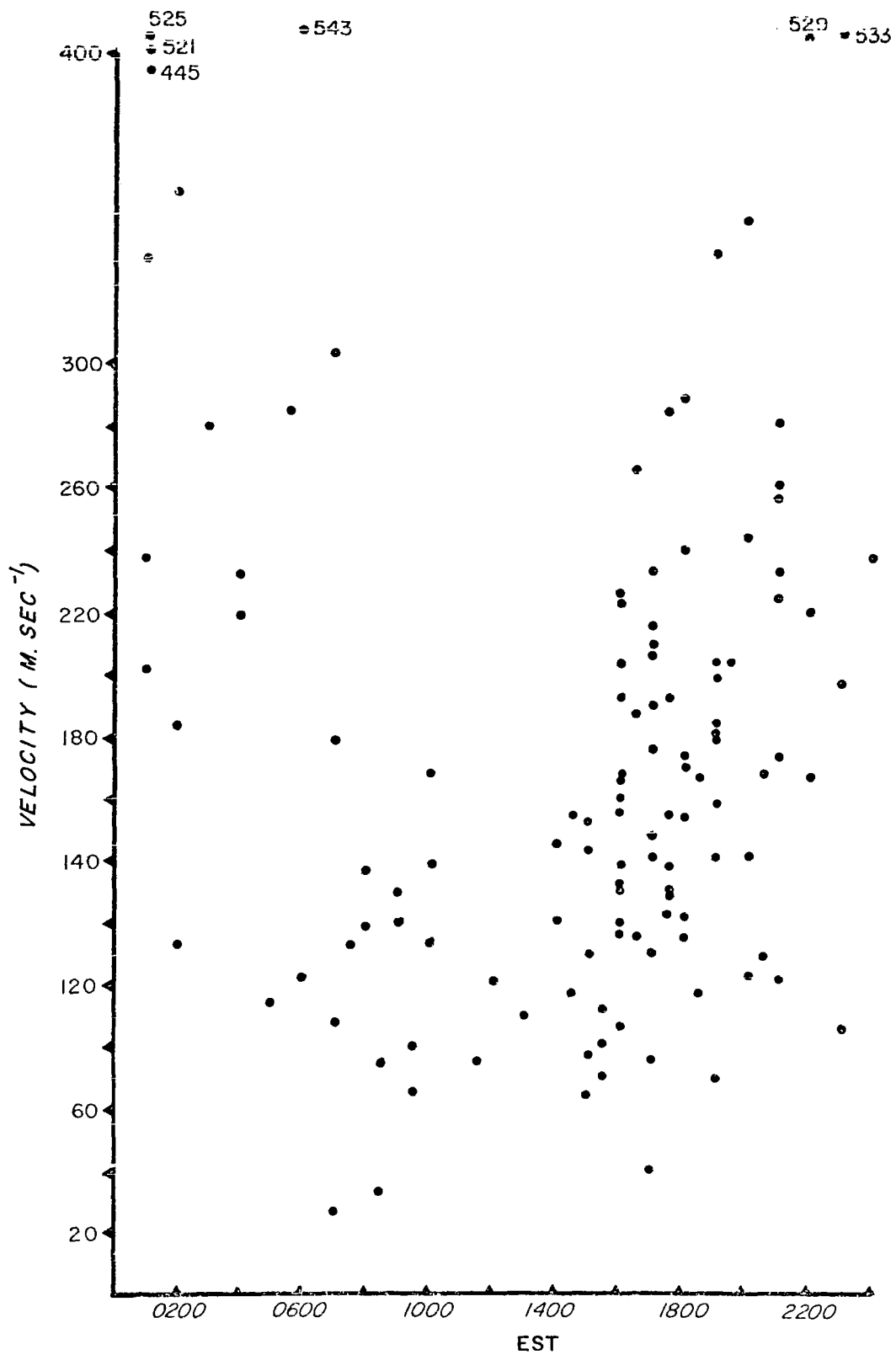
Figure 7: Diurnal variation of TID velocities.

52

Figure 8: Diurnal variation of TID directions
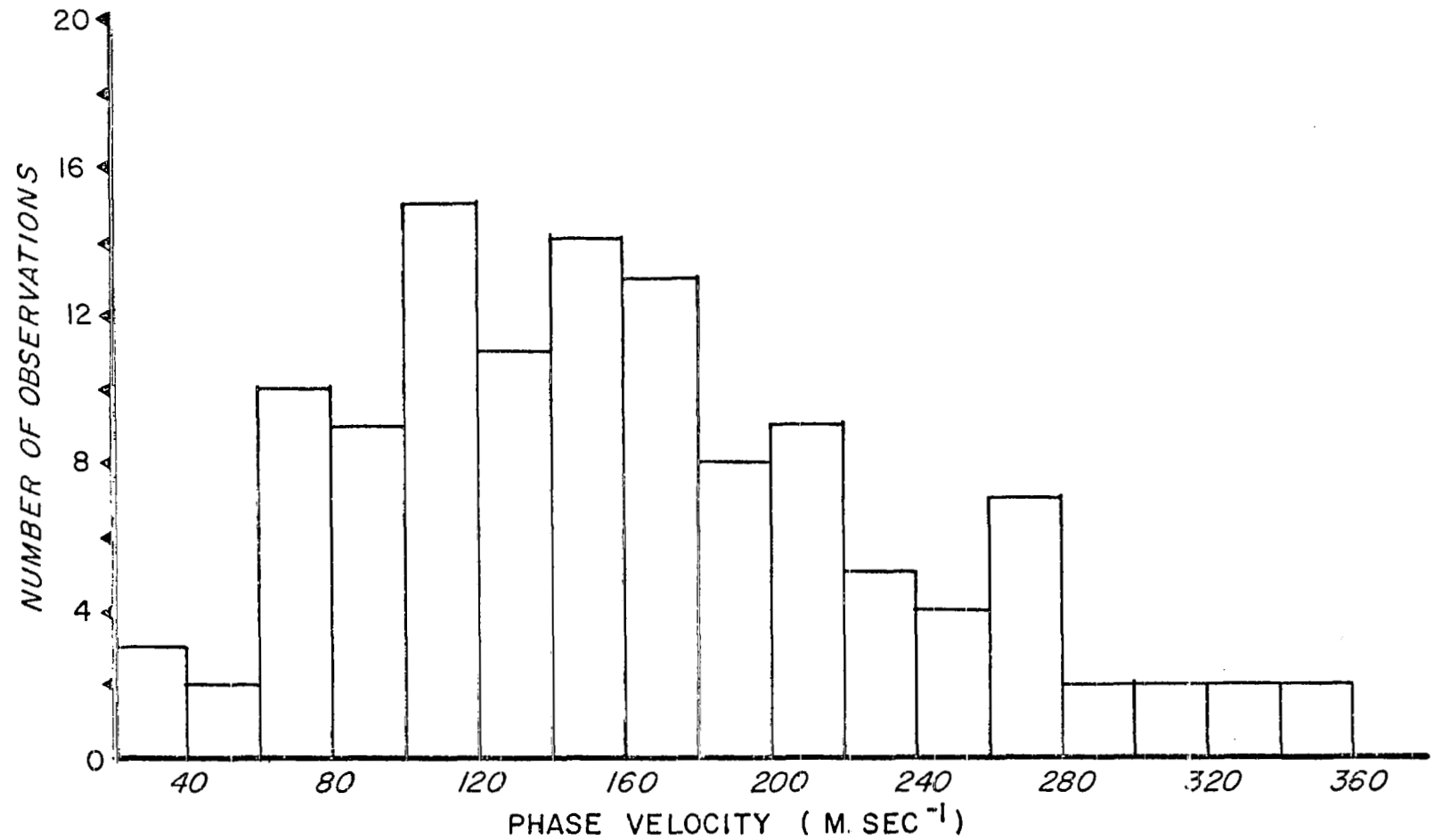
Figure 9:  Histograms for TID velocities.
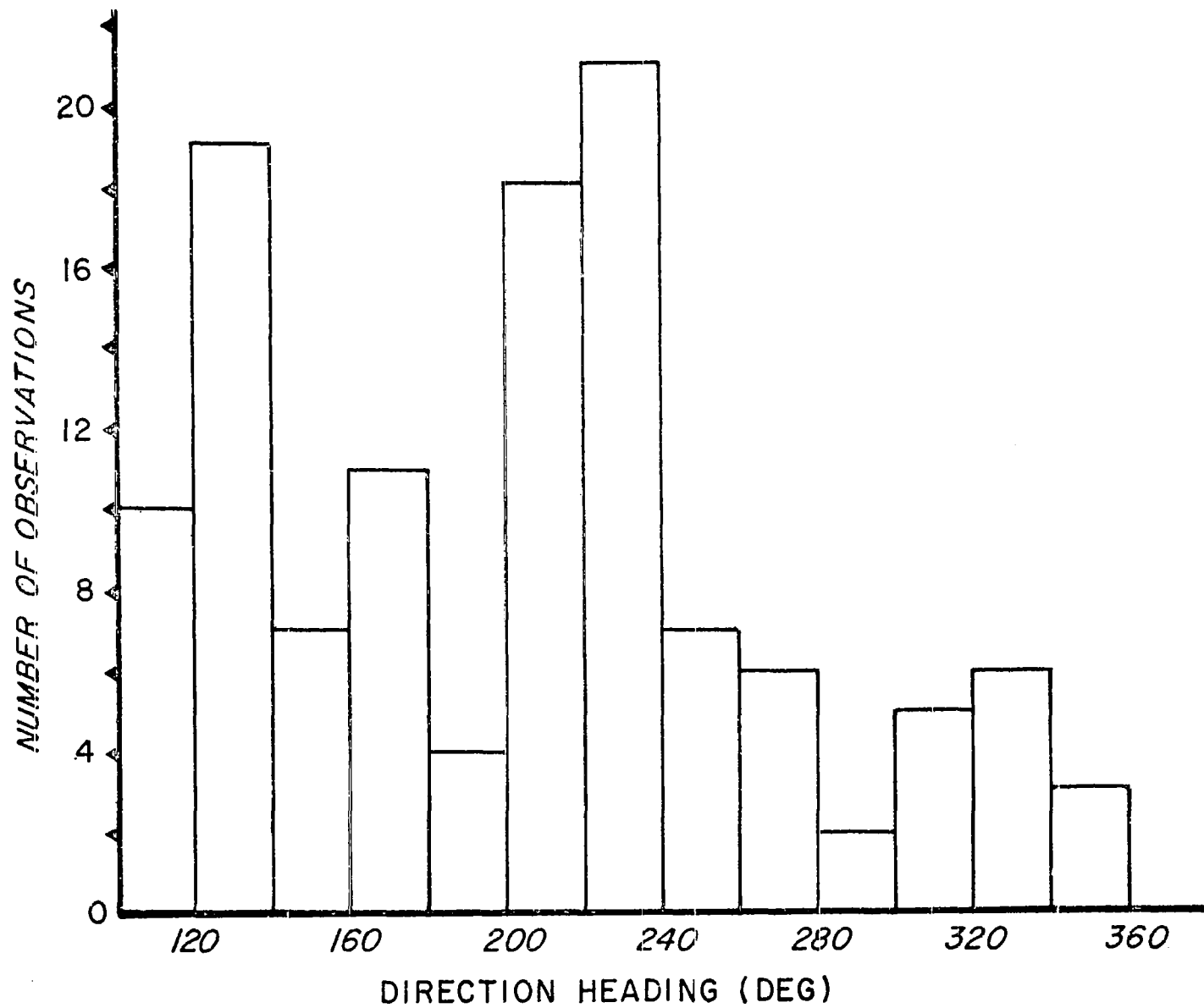
Figure 10:   Histograms for TID directions.
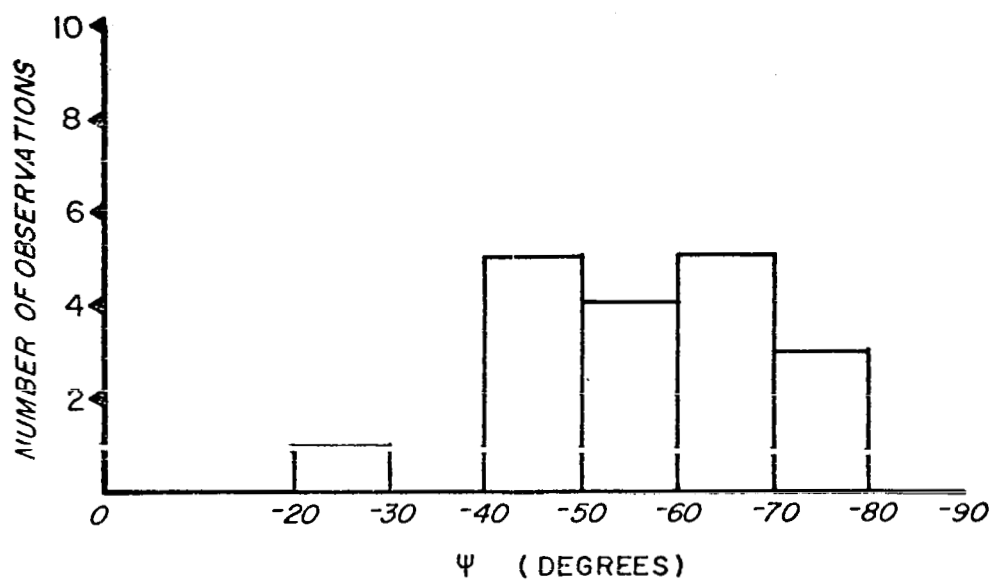
Figure 11:   Histograms for ψ.
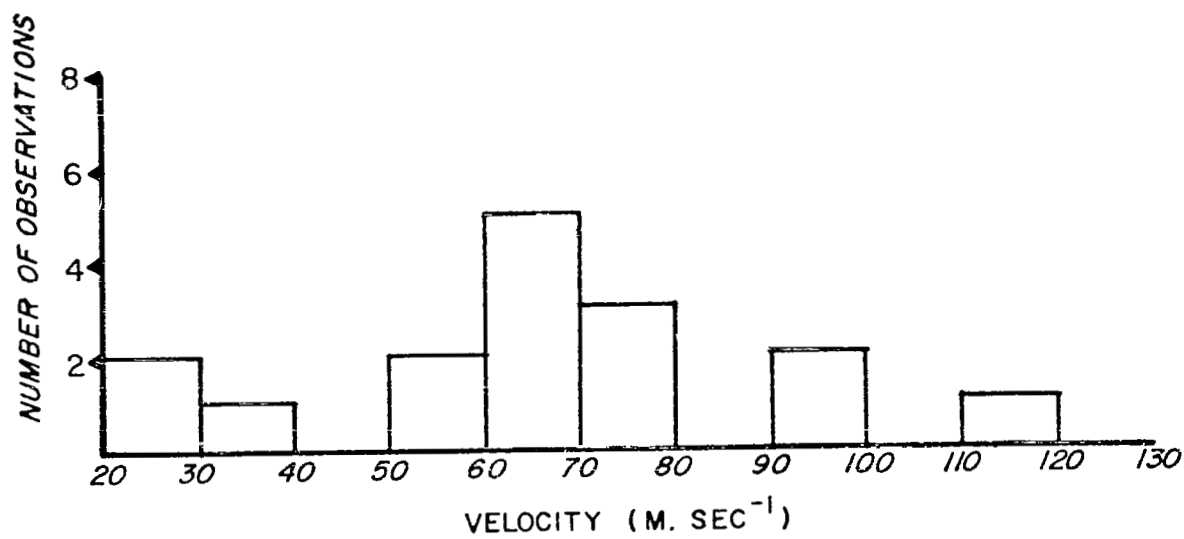


Figure 12:   Histograms for three dimensional TID velocities.

WESTWOOD

THORNHURST

CATSKILL

1 HZ

Lift off of
Apollo XII

LEBANON

1100        1200        1300        1400
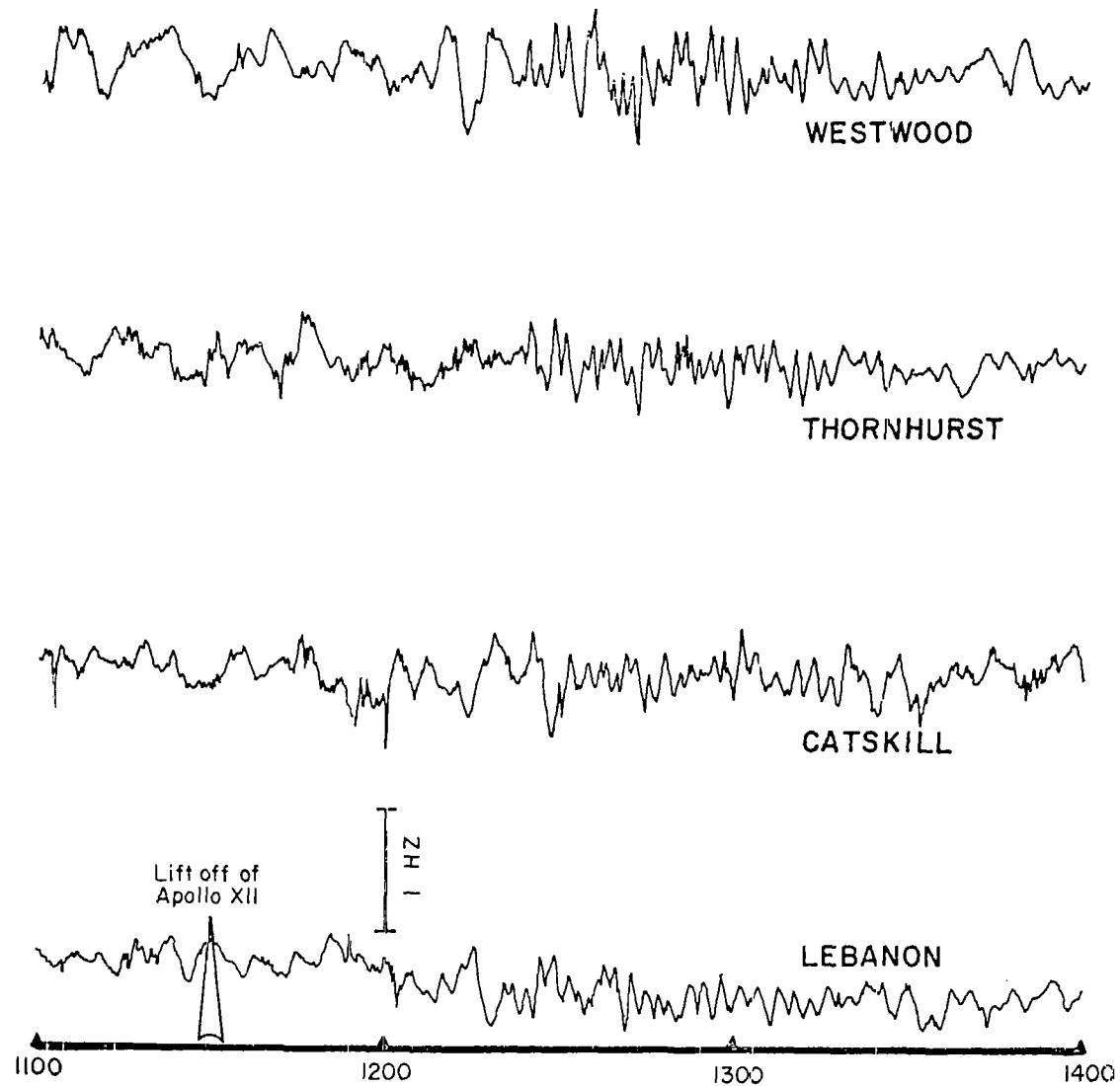
Figure 13:   Apollo 12 signal as seen on a CW doppler record.

Figure 14:   Cross spectral plots before the
Saturn-Apollo 12 signal.

58

# DOPPLER LEB X DOPPLER WESTWOOD

## NOV. 14 1969 1220 TO 1340 EST

### PERIOD (MIN)
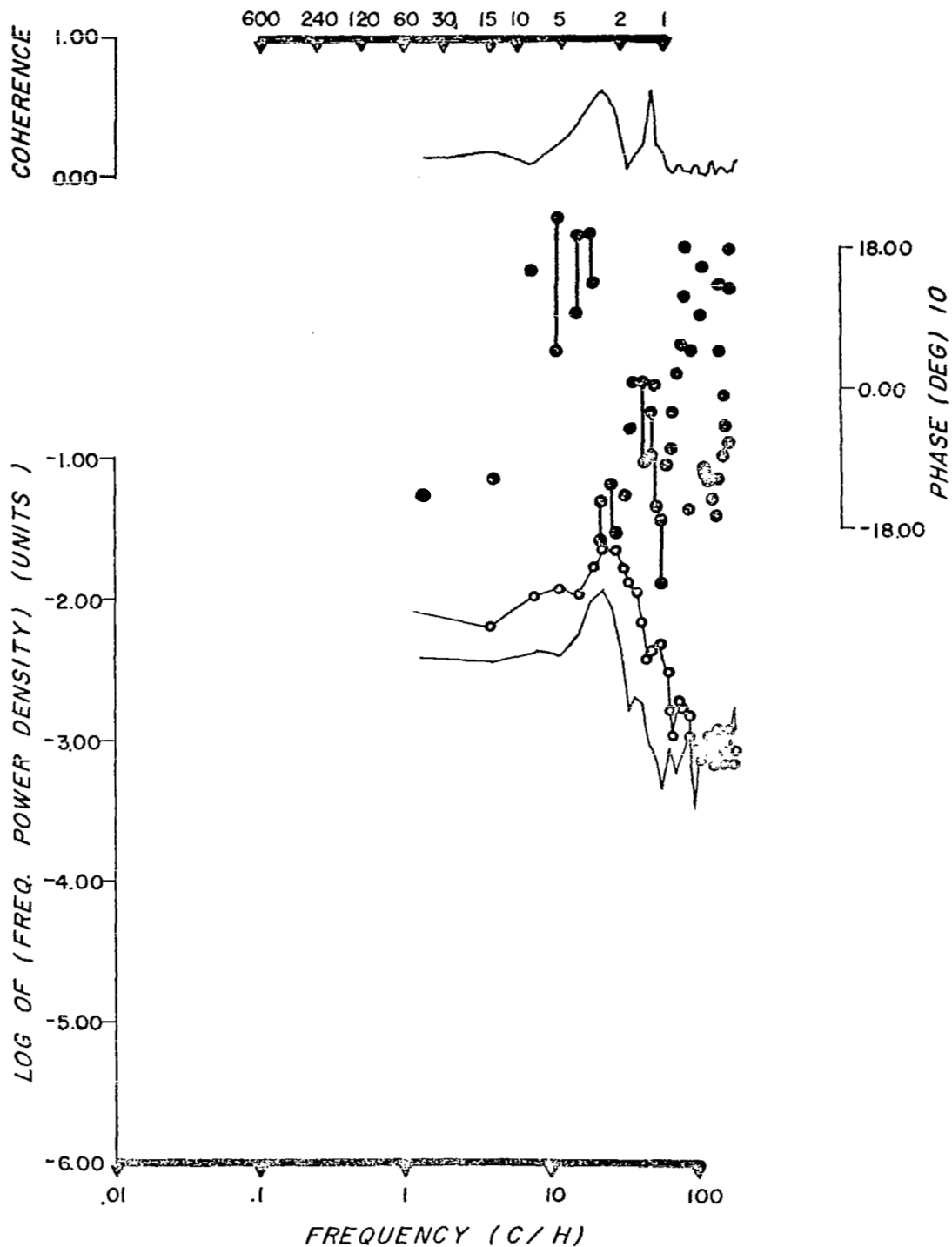


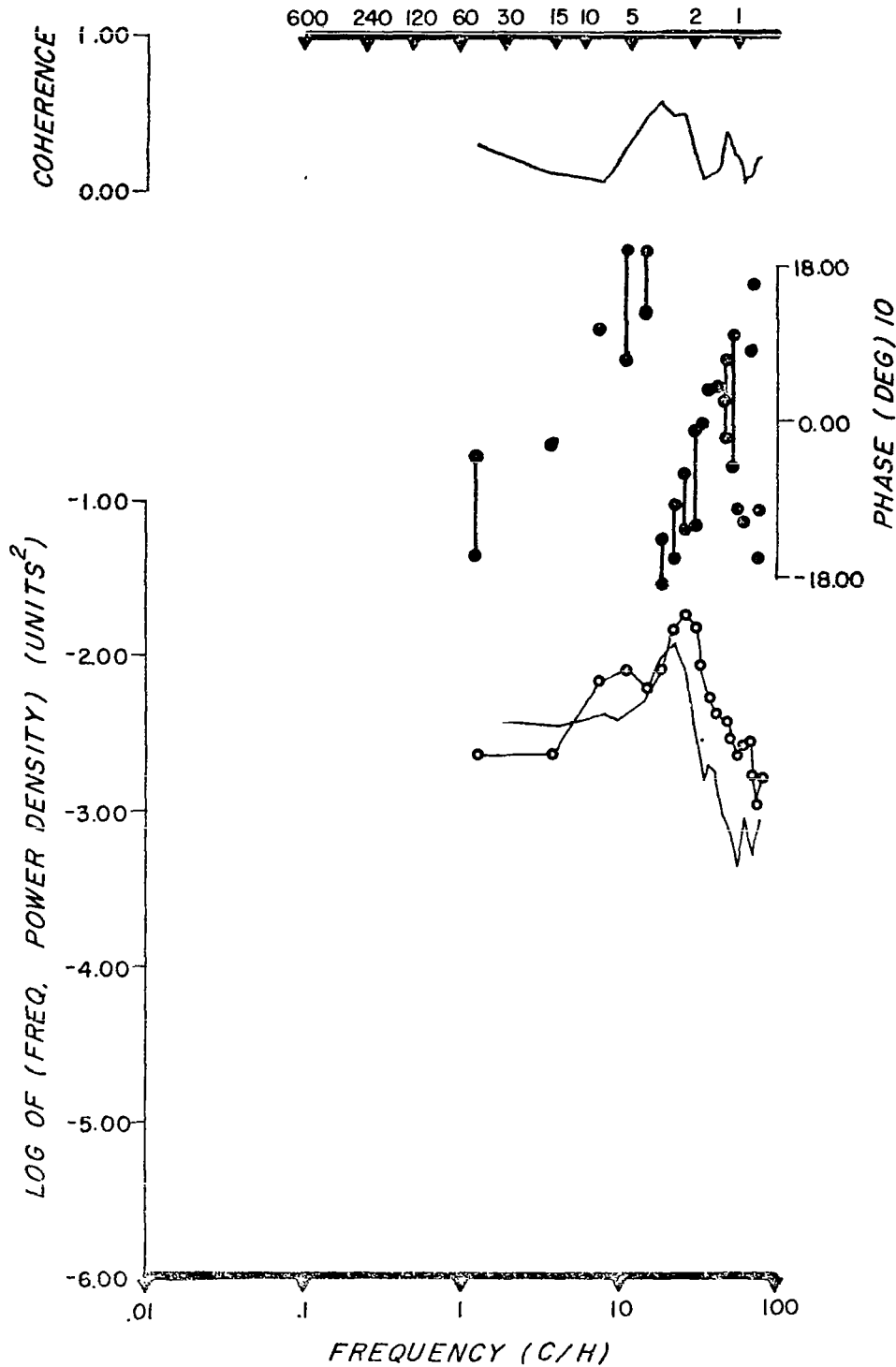Figure 15:   Cross spectral plots between Lebanon and Westwood

Figure 16: Cross spectral plots between Labanon and Thornhurst.

# DOPPLER CATS X DOPPLER THORN
## NOV. 14 1969 1220 TO 1340 EST



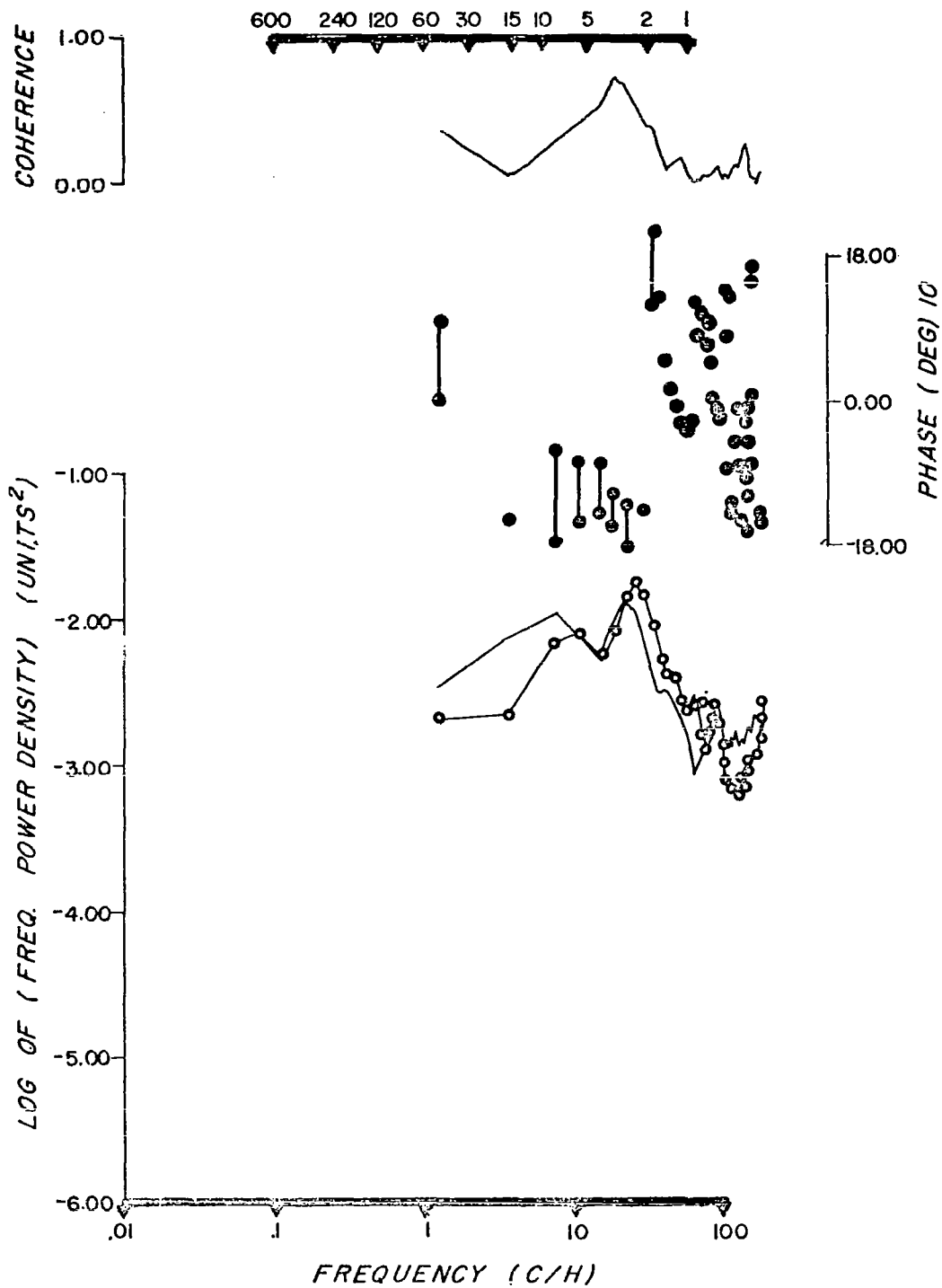Figure 17:    Cross spectral plots between Catskill and Thornhurst.

DOPPLER 6.0 MHZ
WESTWOOD

DOPPLER 4.8 MHZ
WESTWOOD

DOPPLER 4.8 MHZ
THORNHURST

DOPPLER 4.8 MHZ
CATSKILL

1208

DOPPLER 4.8 MHZ
LEBANON

0.5 hZ

1100    1130    1200    1230    1300    1330
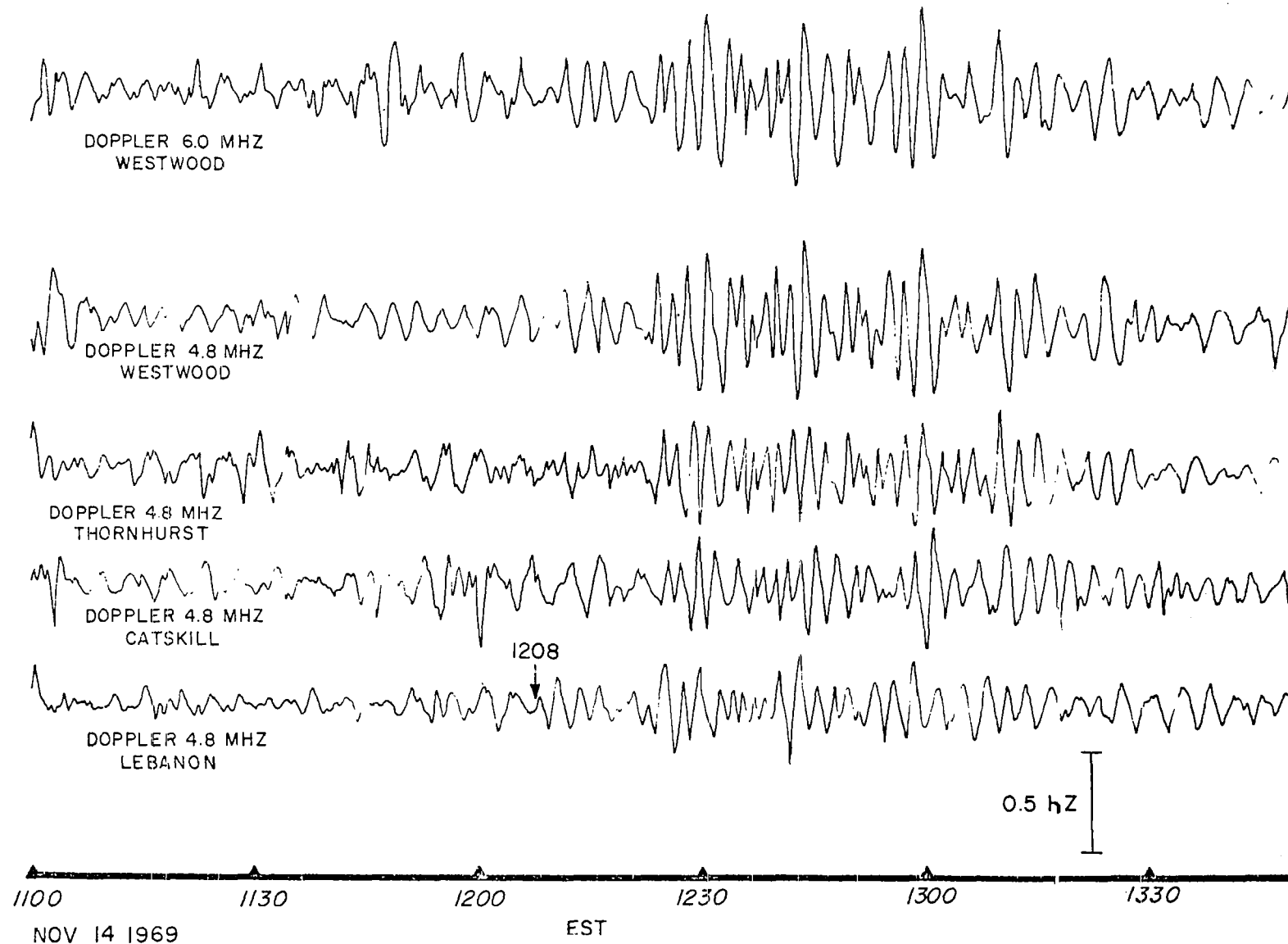
NOV 14 1969                    EST

Figure 18:   The 1-5 min bandpass filtered CW doppler record showing
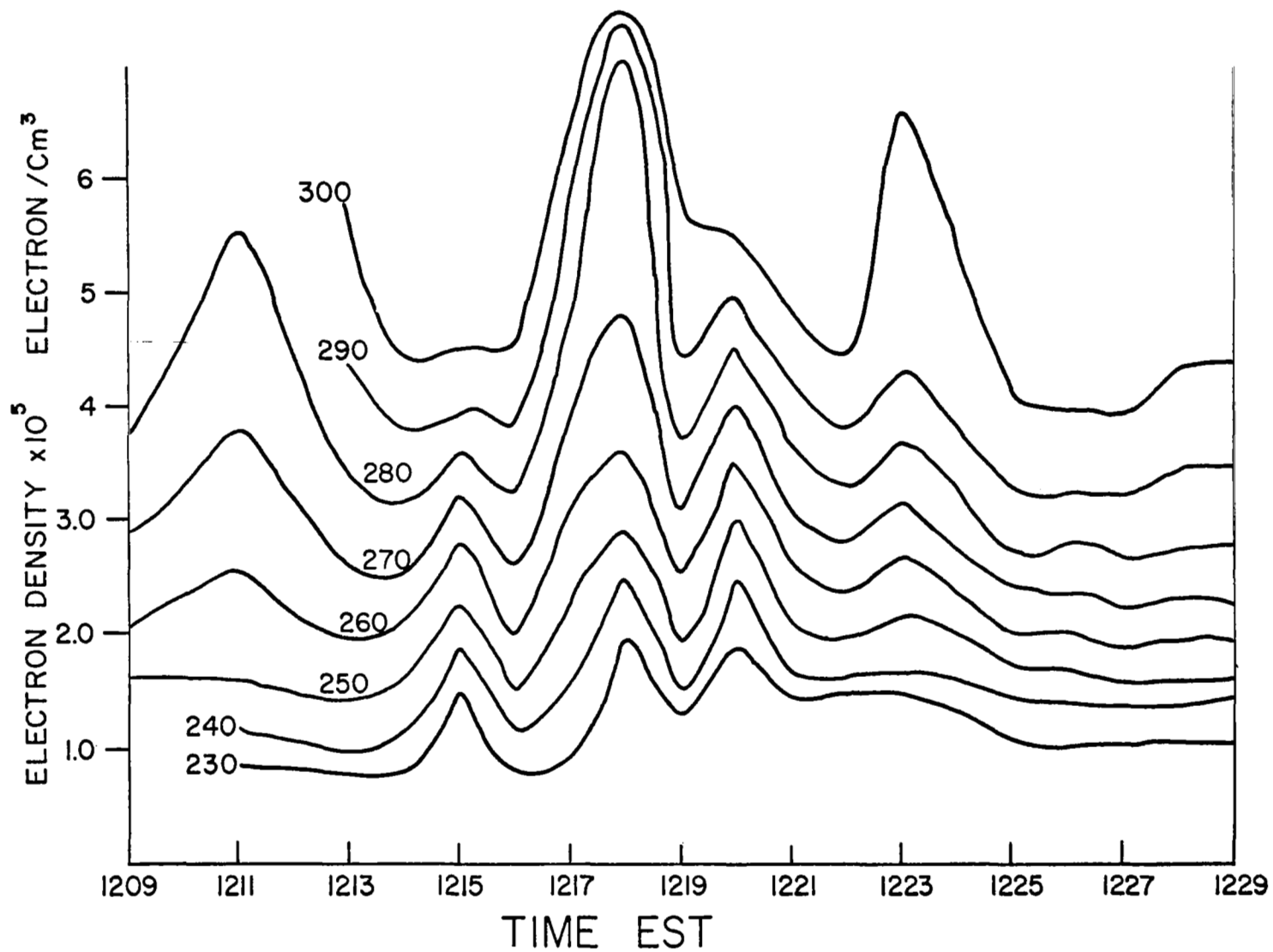             Saturn-Apollo 12 signal.

62

Figure 19: Diagram of electron density contours for Apollo 12.